Akademie věd
České republiky

Teze disertace

k získání vědeckého titulu "doktor věd"

Chemické vědy

ve skupině věd ……

Sulfide Hydrotreating Catalysts by Solvent Assisted Spreading

…….

název disertace

Chemické inženýrství

Komise pro obhajoby doktorských disertací v oboru …….

Mgr. Luděk Kaluža, Ph.D.

Jméno uchazeče ……

Ústav chemických procesů AV ČR, v. v. i.

Pracoviště uchazeče ……..

Praha, 1. března 2018

Místo a datum ……..

Resume

The specific and original features of the present thesis lie in a novel method of preparation of heterogeneous catalysts. This method has been called Slurry Impregnation or alternatively **Solvent-Assisted Spreading (SAS)** and attracts the author´s attention systematicaly and long term. This thesis is the first report that summarizes a novel methodology of the preparation of Co(Ni)Mo catalysts to demonstrate thier activity and selectivity in model **hydrotreating reactions** such as hydrodesulfuritazion (HDS) or hydrodenitrogenation (HDN). The original method, SAS, has been successfully applied for deposition onto various and novel supports. The prepared catalysts were evaluated in terms of reaction progress kinetic analysis (to determine the weight or volume based activities) and, wherever sensibly possible, structural (X-ray diffraction, Raman spectroscopy), textural (nitrogen physisorption) or transport (inverse gas chromatography) characterization. The present thesis thus contributes to the comprehensive and increasingly growing subject heterogeneous catalysis of the field of chemical engineering, wherein **catalysis over sulfides** represents a fundamental role.

More specificaly, the SAS method uses precursors of **low solubility** in water such as MoO_3, $CoCO_3$ or $NiCO_3.2Ni(OH)_2$ to prepare supported catalysts instead of high solubility precursors (solubility higher than 40 g per 100 ml of H_2O) such as $(NH_4)_6Mo_7O_{24}$, $Co(NO_3)_2$ or $Ni(NO_3)_2$ typical for other methods of preparation (conventional impregnation). Low solubility (mostly below 0.13 g per 100 ml of H_2O) was found to be sufficient to gradually dissolve the compound and to simultaneously absorb the compound onto support surface. A schematic comparison of the principle of the SAS and conventional impregnation is shown in Table, wherein electrostatic interactions, i.e. point-of-zero charges (PZC) of support or MoO_3 catalyst and pH of the H_2O/precursor slurry, schematically explain the possible driving forces of the SAS method. The SAS method has been shown to be suitable in the deposition of MoO_3 onto supports such as Al_2O_3, AlOOH, ZrO_2, $ZrO(OH)_2$, TiO_2, C, MgO, and SiO_2-Al_2O_3. It has been also concluded that Co and Ni can be deposited over catalysts containing a saturated adsorption monolayer of MoO_3 by SAS, i.e. from aqueous slurries of low solubility carbonates or hydroxycarbonates. The SAS method does not make it possible to exceed the dispersion capacity of the support surface or to form three dimensional (bulky), and therefore catalytically inactive, phase on the support. This method is a clean and simple method of Co(Ni)Mo deposition, which does not introduce any auxiliary ions like NH_4^+ or NO_3^-; furthermore, calcination is not needed. Avoiding the calcination step is particularly important on preparing of the C supported catalysts due to their propensity to burn. Methanol instead of water is used as a solvent during the impregnation of hydrothermally unstable supports MgO and mesoporous organized Al_2O_3. Only water or methanol is produced on drying. Water or methanol represent the only side products of the SAS. The SAS method thus belongs to the group of **green chemistry** and conforms to **sustainable development**.

Schematic principles of SAS and conventional impregnation

Features of impregnation mixtures			Features of substrates		Features of prepared catalysts	
Precursor	Solvent	pH[a]	Support/Catalyst	PZC[a]	Composition after drying	PZC[a]
Solvent-Assisted Spreading (SAS) techniques (from slurries):						
Water-Assisted Spreading						
MoO_3(s)	H_2O	2.5	Al_2O_3	7	MoO_3/Al_2O_3	2.5
$CoCO_3$(s)	H_2O	8.6	Al_2O_3	7	Spreading does not proceed	
$CoCO_3$(s)	H_2O	8.6	MoO_3/Al_2O_3	2.5	$CoO\text{-}MoO_3/Al_2O_3$	4.0
Methanol-Assisted Spreading						
MoO_3(s)	CH_3OH	-	MgO	12	MoO_3/MgO	2.5
Chelating Agent Assisted Spreading:						
NTA(s),$CoCO_3$(s),MoO_3(s)	H_2O	1.0	Al_2O_3	7	$NTA\text{-}CoO\text{-}MoO_3/Al_2O_3$	
NTA(s),$CoCO_3$(s),MoO_3(s)	$(CH_3)_2SO$	-	MgO	12	$NTA\text{-}CoO\text{-}MoO_3$/MgO	
Conventional impregnation techniques (from true solutions): [b]						
$(NH_4)_6Mo_7O_{24}$(dis)	H_2O	7.5	Al_2O_3	7	$MoO_3\text{-}(NH_4)_6Mo_7O_{24}/Al_2O_3$	
$Co(NO_3)_2$(dis)	H_2O	6.9	MoO_3/Al_2O_3(Calcined)	2.5	$CoO\text{-}Co(NO_3)_2\text{-}MoO_3/Al_2O_3$	
NTA,$Co(NO_3)_2$,$(NH_4)_6Mo_7O_{24}$ [c]	H_2O	-	Al_2O_3	7	$CoMoO_xN_yH_z/Al_2O_3$	

Notes: [a] the values of pH and PZC are valid only in H_2O

[b] vast variety of modifications not shown

[c] alternatively MoO_3 and/or NTA is dissolved in H_2O and a surplus of NH_4OH to make solution

It has been shown on investigations the shaped form of support that an eggshell radial profile of Mo concentration is formed by SAS. The thickness of the eggshell can be efficiently regulated by the amount of MoO_3 used. MoO_3 is adsorbed as a well defined monolayer in the shell. Homogenous concentration profile of MoO_3 (staruration of entire body of support) can be done and oversaturation of support is not principaly possible by SAS. Moreover, CoMo and NiMo active phases can also be added to an α-boehmite paste, using the principles of SAS, before shaping. The sequential reaction of α-boehmite with MoO_3 and then Co or Ni carbonates in an aqueous paste leads to an increased textural stability of Al_2O_3 during calcination. The catalysts prepared by SAS are at least as active and selective in model HDS reactions as the reference commercial or conventionally prepared counterparts.

The SAS was also successfully modified using a chelating agent to avoid an addition of surpluses of NH_4OH, which is usually used in convetional preparations. Increased HDS activities were observed. The first attempt was done also for a deposition of PtO_2 over carbon blacks supports instead of conventionally used H_2PtCl_2 to prepare fuel cell electrocatalysts.

It was concluded that specific chemistry of each individual supports and catalysts such as content of Na, Ca, or Cl admixture (the sample history), as well as structural, textural and transport parameters such as crystal structure, surface area, microporosity, mean transport pore radii are the key factors to monitor carefully in order to prepare heterogeneous catalysts active and selective in a particular reaction.

Acknowledgements

Author kindly acknowledges supervisors Ing. Rudolf Peter, CSc. and Ing. Miroslav Zdražil, DrSc. who introduced fundamentals of scientific work during his elaborations on Mgr. and Ph.D. theses, respectively. Later, the long-term experience of Dr. Zdražil in the field of heterogeneous catalysis was especially helpful for continuation of the spirit of sulfidic group to advance the specific insight on sulfides [O1-O13, O15-O20, O22-O24]. Dr. Zdražil and Ing. Magdalena Bendová, Ph.D. are also acknowledged for proofreading of this text.

During his scientic carrier comprising more than 50 original papers, the author cooperated with plenty of coauthors as it is usual in the field of heterogeneous catalysis. More specifically, 25 original papers are included in the present thesis, wherein the author is present 18 times as a first author, 15 times as a corresponding author, 14 times as a first author as well as cooresponding author, and 1 time as a single author. In other papapers [1-27], the author contributes as 7 times as a first author, 5 times as a corresponding author and 3 times as a first author as well as cooresponding author. The kind acknowledgement of the below mentioned technical supports must be devoted to Prof. Ing. Jiří Čejka, DrSc., and Ing. Naděžda Žilková for providing samples of organized mesoporous alumina [O17, 1,2]; Ing. David Kubička, Ph.D, MBA, for determination of catalyst activity in rapeseed oil hydrorefining [3,4]; Mikkel Juul Larsen, Ph.D., and Madeleine Odgaard, MSc., for determination of electrocatalyst activity in oxygen reduction reaction [5-7]; Prof. Georgi Tyuliev, Ph.D., or Alla Spojakina, Dr., or Ing. Květuše Jirátová, CSc., for x-ray photoelectron spectroscopy, infrared spectroscopy and synthesis of sulfides prepared by Co or Ni polyoxomolybdates [8-12]; Ing. Václav Novák, CSc., for determination of catalyst activity in hydrodesulfurization of light gas oil in pilot plant [9]; Ing. Olga Šolcová, DSc. and Ing. Karel Soukup, Ph.D. for static nitrogen physisorption and determination of textural and transport characteristics [O17,O23,O25]; Ing. Petr Žáček, Ph.D., Mgr. Jindřich Karban, Ph.D., Ing. Jan Storch, Ph.D., and Ing. Jan Sýkora, Ph.D, for isolation and analysis of isomers of methylcyclohexenes [13]; Doc. Mgr. Roman Maršálek, Ph.D., for zeta potential measurement; Ing. Martin Koštejn, Ph.D., for Raman spectroscopy measurement [O23]; Ing. Pavel Topka, Ph.D. or Ing. Jana Gaálová, Ph.D. for the measurement of VOC oxidation reactions [14-17] or and Ing. Zdeněk Vít, CSc., or Ing. Daniela Gulková, CSc., for determination of catalyst activity in cumene cracking and 4,6-dimethyl-dibenzothiophene hydrodesulfurization reactions or TPR [O3,O4,O6-O9, O13, O14,O17-O20, O22, 19-27].

The companies BASF (Germany), Albemarle (The Netherlands), and Shell (The Netherlands), are acknowledged for providing the reference catalysts Mo/Al_2O_3, and $CoMo/Al_2O_3$ and $NiMo/Al_2O_3$. The companies Norit b.v. (The Netherlands) and Slovenské lučobné závody (Slovak Republic) are acknowledged for providing activated carbons. MEL Chemicals (England) is acknowledged for providing $ZrO(OH)_2$. Eurosupport Manufacturing Czechia is acknowledged for providing TiO_2.

Acknowledgements of financial support

As a principal investigator, the author thanks for financial support to Czech Science Foundation for the postdoctoral project with grant no. 104/06/P034 [O9, O10, O11, O12, O14, O15, O16, 9], standard grant projects with grant nos. P106/11/0902 [O18, O19, O20, O21, O22, O23, O25, 8, 11-14, 19, 20, 26-28] and 17-22490S [O24, 4], and to European Union´s 7th Framework Programme through the Fuel Cells and Hydrogen Joint Undertaking Technology Initiative with grant no. 303466 (IMMEDIATE) and the co-financing of the Ministry of Education, Youth and Sports of the Czech Republic with grant no. 7HX13003 [O23, 5-7].

As a member of research teams, the author thanks for financial support to Grant Agency of Academy of Science of the Czech Republic, grant nos. A4072802 [O1], A4072103 [O3, 24], IAA4072306 [O4, O5, O6, O8], and to Czech Science Foundation, grant nos. 104/01/0544 [O2, 1,2], 104/06/0705 [O7, O9, O13, O16, 22], and 104/09/0751 [O17, 10, 18-20, 23, 25, 26].

Thanks to the projects Open Science, the author has been continuously training pre-graduate students as a lector since 2005. Three talented students selected from seven of these projects Martin Procházka [O25], Kateřina Smítalová, and Jan Moravčík also joined our sulfidic group to solve above mentioned standard scientific projects of Czech Science Foundation. Thanks to Open Science, our workplace thus, with advantage of future outlook, performs both cultured public relation activities and an intelligent human resources management.

1. Introduction

Typical sulfidic heterogeneous catalysts developed for industrial hydrotreating (hydrorefining, hydroprocessing) reactions over the past 70 years are based on $CoMoS_x/Al_2O_3$, $NiMoS_x/Al_2O_3$ and $NiWS_x/Al_2O_3$. [29] Quite recently, also an unsupported form of Co(Ni)MoW sulfides have been applied industrially. [30] The typical hydrotreating reactions comprise hydrodesulfurization (HDS), hydrodenitrogenation (HDN) and hydrogenation (HYD). The increasingly actual urgency of research onto new sulfidic catalysts is driven by: i) continuous pressure of legislation on virtually zero level of S in transportation fuels (to limit the SO_x, NO_x and particulate matter pollutants), ii) processing of heavier and more sour (S rich) petroleum crudes, iii) changes in feeds, i.e. more processing of low value stocks such as visbreaker oil or stocks coming from fluid catalytic cracker (FCC), particularly light cycle oil and heavy stocks of FCC (the typical hydrotreating reactions are accompanied with olefin hydrogenation reaction, HYDO), iv) co-upgrading of environmentally sustainable biofeedstocks such as biooils by hydrodeoxygenation (HDO). [31] Sulfur removal (and very deep removal) by HDS in all kind of hydrocarbon streams will still be a requirement over the coming 30 to 40 years and research in this area of hydrotreating is essential. The importance of novel catalyst development to handle with the sulfur removal and, therefore, the importance of fundamental research of novel catalysts is naturally underlined by the fact that changing of process parameters or building novel investment unit is not always reasonable.

Nonetheless, MoO_3 based catalysts, which are mostly addressed in the present work, are also used in other reactions than hydrotreating. The promising catalytic activity has been verified in a variety of catalytic applications, such as total methane oxidation [32], partial oxidation of methane [33], partial oxidation of methanol [34,35], epoxidation of propylene [36], partial oxidation of propylene[37], selective oxidation of 1-butene and butadiene [38], ammoxidation of toluene [39,40], ammoxidation of 3-picoline [41], water-gas shift [42], epoxidation of allylacetate with 3-butyl hydroperoxide [43,44], selective reduction of NO_x by NH_3 [45-48], anaerobic oxidation of butane to butadiene [49], oxidative dehydrogenation of ethylbenzene [50], butane [51] or propane [52,53], metathesis of propene [54,55,56-58], wet oxidation of H_2S to sulfur [59], hydrogenation of carbon monoxide and toluene [60], heptane isomerization [61], ethane and ethene homologations [62,63], methane dehydroaromatization [64], toluene benzoylation [65], alkylation of benzene with aliphatic alcohols [66,67], 2-propanol dehydrogenation and cumene dealkylation [68], or 2-butanol dehydration and esterification of acetic acid with ethanol [69]. The catalysts discussed in the present work thus overwhelm the field of sulfidic hydrorefining catalysis.

Recent scientific effort to investigate novel catalysts is focused on new supports, new active phases and new methods of preparation. Two of these aspects, novel and original preparation method and novel supports, are discussed below. The novel method of catalysts preparation called Slurry Impregnation or alternatively Solvent-Assisted Spreading (SAS) attracted systematic and long term author´s attention. To the best of the author´s knowledge, this thesis is the first report summarizing the novel methodology of preparation of Co(Ni)Mo catalysts to demonstrate its superior selectivity to gain highly dispersed and active catalysts.

2. Solvent-Assisted Spreading (Slurry impregnation)

The specific and original features of SAS method is that it uses precursors of low solubility in water such as MoO_3, PtO_2, $CoCO_3$ or $NiCO_3.2Ni(OH)_2$ for the preparation of supported catalysts instead of high solubility precursor such as $(NH_4)_6Mo_7O_{24}$, H_2PtCl_6, $Co(NO_3)_2$ or $Ni(NO_3)_2$ typical for other methods of preparation. The low solublity was found to be sufficient for gradual dissolution of a compound and adsorption onto support surface. A schematic overview comparing principle of SAS and conventional impregnation is shown in Table 1. The SAS method has been novely and successfully applied to impregnate the

supports Al_2O_3, α-AlOOH, ZrO_2, $ZrO(OH)_2$, TiO_2, C, MgO, and SiO_2-Al_2O_3. The first atempt was done also for deposition of PtO_2 over carbon blacks supports. The sections below analyze the character of MoO_3 deposition, concept of of Co and Ni depostions, modification of SAS with chelating agent, and specific feature of each individual support with relation to neccesasary characterization techniques and empiric reaction progress kinetic analysis for determination of activity and selectivity.

Table 1: Schematic principles of SAS and conventional impregnation

Features of impregnation mixtures			Features of substrates		Features of prepared catalysts	
Precursor	Solvent	pH[a]	Support/Catalyst	PZC[a]	Composition after drying	PZC[a]
Solvent-Assisted Spreading (SAS) techniques (from slurries):						
Water-Assisted Spreading						
MoO_3(s)	H_2O	2.5	supp.[b]	7	MoO_3/ supp.[b]	2.5
$CoCO_3$(s)	H_2O	8.6	supp.[b]	7	Spreading does not proceed	
$CoCO_3$(s)	H_2O	8.6	MoO_3/Al_2O_3	2.5	CoO-MoO_3/ supp.[b]	4.0
Methanol-Assisted Spreading						
MoO_3(s)	CH_3OH	-	MgO or OMA[c]	12 or 7	MoO_3/MgO or OMA[c]	2.5
Chelating Agent Assisted Spreading:						
NTA(s),$CoCO_3$(s),MoO_3(s)	H_2O	1.0	supp.[b]	7	NTA-CoO-MoO_3/ supp.[b]	
NTA(s),$CoCO_3$(s),MoO_3(s)	$(CH_3)_2SO$	-	MgO	12	NTA-CoO-MoO_3/MgO	
Conventional impregnation techniques (from true solutions): [d]						
$(NH_4)_6Mo_7O_{24}$(dis)	H_2O	7.5	supp.[b]	7	MoO_3-$(NH_4)_6Mo_7O_{24}$/ supp.[b]	
$Co(NO_3)_2$(dis)	H_2O	6.9	MoO_3/ supp.[b] (Calcined)	2.5	CoO-$Co(NO_3)_2$-MoO_3/ supp.[b]	
NTA,$Co(NO_3)_2$,$(NH_4)_6Mo_7O_{24}$[e]	H_2O	-	supp.[b]	7	$CoMoO_xN_yH_z$/ supp.[b]	

Notes: [a] the values of pH and PZC are valid only in H_2O
[b] supp. = Al_2O_3, α-AlOOH, ZrO_2, $ZrO(OH)_2$, TiO_2, C, and SiO_2-Al_2O_3
[c] OMA = organized mesoporous Al_2O_3
[d] vast variety of modifications not shown
[e] alternatively MoO_3 and/or NTA is dissolved in H_2O and a surplus of NH_4OH to make solution

2.1. Mo catalysts and concept of MoO_3 monolayer

Preparation of Mo supported catalysts is mostly based on conventional impregnation of a support with true solution of a metal salt. The Mo precursor, solvent, additives, conditions of drying, calcination and activation govern resultant catalyst activity and selectivity. The preparation of typical MoO_3/Al_2O_3 includes impregnation of the support with solution of well soluble $(NH_4)_6Mo_7O_{24}$ by pore filling method or by impregnation of the support from the excess of the impregnation solution (the volume of the solution is higher than the support pore volume). Part of the Mo species is adsorbed onto the support surface during the contact of the support with impregnation solution. The adsorption is not very strong and the adsorption amount is not very high because the natural pH of the impregnation solution is about 6-8, which is close to point of zero charge (PZC) of Al_2O_3. Other part of Mo species precipitates in the pores of the support during drying. These species remain in bulk (three dimensional crystalline phase) if conditions of calcinations are too mild. More severe condition of calcination results in spreading of MoO_3 species to form other portion of monolayer coverage (the wanting form of Mo) but causes also formation of bulky $Al_2(MoO_4)_3$.

The exact chemistry of Mo monolayer has been subject of numerous papers and it shall not be discussed in the present work. Depending on the loading and pH, chemical interactions of various strengths, ranging from condensation reactions with surface oxygen

containing groups to electrostatic interactions with coordinatively unsaturated sites, are involved. The density of structures capable of chemical interactions (various types of OH groups, Al^{3+} sites) is large enough to achieve the formation of a monolayer of molybdena species on alumina supports. The formation of monomeric tetrahedral molybdates at low loadings of Mo and polymeric octahedral molybdates at higher loadings of Mo during conventional impregnation were reported elsewhere [70-72]. Nonetheless, the amount of $(NH_4)_6Mo_7O_{24}$ needed for the given Al_2O_3 to form monolayer must be determined experimentally in advance. For example, X-ray diffraction analysis (XRD) is done over a set of samples with different loading of MoO_3. Bulk (crystalline) MoO_3 or $Al_2(MoO_4)_3$ are detected when the condition of preparation are not eligible.

In contrast, the monolayer form of Mo has been related to the best catalytic performance. The monolayer Mo species are sulfided to well dispersed MoS_2 slabs in sulfide Mo, CoMo and NiMo catalysts while bulk MoO_3 is the precursor of large MoS_2 crystals of low hydrotreating activity [29,73]. The best catalytic performance has been reported, for example, in oxidative dehydrogenation of ethane over highly dispersed two-dimensional Mo species fully encapsulating the alumina surface [74]. Furthermore, the filled monolayer, i.e. the monolayer wherein the surface of support is just covered by Mo species, represents the most convenient form. At the Mo loading lower than the loading of the filled monolayer, the capacity of support to disperse Mo is not fully utilized and the uncovered support may negatively influenced the catalytic reaction. At the Mo loading higher than the loading of the filled monolayer, the capacity of support to disperse Mo is fully spent. The excess of Mo tend to form bulk MoO_3, being not completely accessible for catalytic reaction.

The equilibrium adsorption method represents another method of deposition of $(NH_4)_6Mo_7O_{24}$ from aqueous solution of the compound. The support is in contact with the impregnation solution at controlled condition and then it is removed and dried. Mo species are deposited by adsorption and the precipitation during drying is thus not extensive [75,76]. However, the problem is the preparation of the filled monolayer catalyst. In order to promote adsorption and to achieve saturated adsorption loading corresponding to filled monolayer, it is necessary to decrease pH of impregnation solution by the addition of acid. Solubility of $(NH_4)_6Mo_7O_{24}$ decreases with decreasing pH and it is difficult to find a proper combination of the concentration and pH to achieve just filled monolayer. At not sufficiently low pH and not sufficiently high $(NH_4)_6Mo_7O_{24}$ concentration, the saturated adsorption loading is lower than filled monolayer loading. At too low pH and too high concentration, the adsorption is accompanied by precipitation of MoO_3 in pores that may pass undetected [72]; precipitation cannot be distinguished from adsorption by the adsorption experiment alone.

The solvent-assisted spreading (SAS) method, alternatively named slurry impregnation [77, O1-O8, O10-O12, O14, O16, O17-O20, O22, O23, O25], is a special case of equilibrium adsorption impregnation. The conditions of SAS are favorable for the formation of well-defined filled monolayer catalyst. For example, it is the reaction of Al_2O_3 support with the MoO_3/H_2O slurry. The natural pH of MoO_3/H_2O slurry is about 2.5, i.e. well below the point of zero charge of Al_2O_3. The adsorption of Mo anions is thus very strong (it is assumed that $Mo_7O_{24}^{6-}$-type anions are present at low pH of the slurry). Simultaneously, there is no thermodynamic driving force for precipitation; the just saturated but not oversaturated solution can be formed in MoO_3/H_2O slurry during SAS.

Filled monolayer catalyst is simply prepared by SAS without any preliminary experiments. Excess of MoO_3 is used and the process of MoO_3 dissolution/adsorption continues until chemical equilibrium is established: chemical potentials of Mo species in solid MoO_3, saturated solution and saturated adsorption monolayer are the same. The saturated adsorption monolayer should be considered as filled monolayer because the chemical potential of the last adsorbed Mo species is equal to the chemical potential of solid MoO_3.

The unreacted MoO_3 is separated from the impregnated Al_2O_3 particles by decantation. The concentration of saturated MoO_3 solution occluded in pores is very low and the amount of MoO_3 precipitated during drying is thus negligible. Calcination of SAS catalysts is not needed (because no NH_3 containing ions are used) and the formation of bulk $Al_2(MoO_4)_3$ is thus avoided. The factors that affect kinetics of SAS of MoO_3 are discussed below in this work.

2.2. Co(Ni)Mo Catalysts - Deposition of CoO (NiO) over MoO_3 catalysts

Similarly to Mo, Co and Ni are conventionally deposited onto supported MoO_3 catalysts by impregnation using true solutions of high solubility salts such as $Co(NO_3)_2$ and $Ni(NO_3)_2$. Conditions of impregnation, drying, calcination, and activation influence resultant properties. In contrast to Mo, the loadings of the Co(Ni) required for efficient promotion of the HDS activity are significantly lower (details are discussed below).

We have introduced SAS method using the low solubility precursors such as $Co(OH)_2$, $CoCO_3.Co(OH)_2$, $CoCO_3$, NiO, $Ni(OH)_2$, $NiCO_3.2Ni(OH)_2.xH_2O$, or $2NiCO_3.3Ni(OH)_2.4H_2O$ [O1, O10-O12, O14, O16, O17, O20, O25] for the ion to react with MoO_3 catalysts in aqueous slurry. During Co(Ni) deposition, part of the pre-deposited MoO_3 may in general dissolve. A saturated solution of molybdic acid can be formed by slurring the catalyst with saturation loading of MoO_3 in water. However, the concentration of this saturated solution is low. The amount of the desorbed MoO_3 is moreover negligible provided that the amount of water is small. Solubility of MoO_3 increases with increased pH. The natural pH of the cobalt (nickel) nitrate impregnation solution is about 5.5 and the dissolution of MoO_3 from MoO_3 catalysts should not be very high during conventional impregnation. In contrast, the natural pH of the Co (Ni) hydroxides carbonates slurry is about 6.7-10.1 and this might promote the dissolution of the deposited MoO_3 during slurry impregnation (see also Section 2.5). However, both in conventional deposition and in slurry deposition of Co (Ni), all contingently dissolved MoO_3 is again redeposited in the drying step, because the impregnation solution and the impregnation slurry is, in principle, not necessary to separate from the impregnated catalyst before drying.

Nevertheless, two conditions seem to be important for the applicability of the SAS to Co (Ni) deposition:

First, the adsorption of the impregnation compound should be strongly preferred thermodynamically. Adsorption of anions is promoted when the natural pH of the impregnation slurry is well below the PZC of the support. This is fulfilled during deposition of MoO_3 onto amphoteric supports such as carbons, aluminas, zirconias and titanias [O1, O2, O5, O6, O7, O12] (see Sections 5 and 6). Adsorption of cations is promoted when the natural pH of the impregnation slurry is well above the PZC of the support. The pH of the slurry of cobalt hydroxide carbonate was about 8.5. That value is not substantially different from the PZC of the supports possessing PZCs of 5-10.1 [O10, O16, O17]. However, it was well above the PZCs of the MoO_3 catalysts with adsorption monolayer of MoO_3, which were about 2.5.

Second, from a kinetic point of view, the solubility of the impregnation compound should not be 'too small'. For example, the solubility of cobalt hydroxide carbonate (solubility product of about 10^{-10} at room temperature) is much lower than solubility of MoO_3 (0.13 g per 100 ml of water at room temperature) [78].

In agreement with those, the SAS of CoO (NiO) is not as easy to accomplish as the slurry deposition of MoO_3. For example, the maximum amount of CoO (NiO) deposited by SAS (saturated adsorption loadings of Co or Ni) are rather small ranging up to about 4 wt.%. In the attempts to prepare catalysts saturated with Co or Ni by SAS, the large amount, surplus, of basic hydroxides carbonates induces desorption of molybdena species from the Mo catalyst, and that fine powder of undeposited $CoMoO_4$ ($NiMoO_4$) is formed as a result. Molybdena from the saturated Mo catalyst is probably more soluble than cobalt hydroxide

carbonate, so the situation can be described as the SAS of cobalt hydroxide carbonate by MoO_3. As it was advised above, this side reaction can be inhibited by using lower amount of Co(Ni) precursors than the saturated adsorption loading is, and using as low amount of solvent as possible. It should be also noted that the amounts of Co (Ni) deposited by SAS are sufficient to promote HDS activity. Other details are discussed below in sections dealing with the supports studied (Sections 5-9).

2.3. Co(Ni)Mo Catalysts - Deposition of CoO (NiO) over MoS_2 catalysts

The newest and original approach of SAS is represented by deposition of $NiCO_3.2Ni(OH)_2$ or $CoCO_3.xH_2O$ onto freshly presulfided Mo species. Water-assisted spreading (slurry impregnation) of $NiCO_3.2Ni(OH)_2$ proceeds onto sulfided surface, in principle, in the same way as the spreading onto oxidic MoO_3/Al_2O_3 surface. The point of zero charge (PZC) of sulfides is often reported to be low of about 2-3 and to be similar to sulfur. Nevertheless, it often depends on the degree of hydrolysis of the sulfides and on partial re-oxidation of the surface [79]. In our experiments, the freshly sulfided Mo catalysts were immersed into distilled water and they exhibited PZC values were about 7, which were stable for some days if the mixture was not stirred. In contrast, after left standing of the sulfided species on air or under vigorous stirring of the sulfide/H_2O slurries, the PZC decreased to about 4. The PZC of 4 should be assumed during slurry impregnation of $NiCO_3.2Ni(OH)_2$ onto sulfide Mo catalysts.

The impregnation $NiCO_3.2Ni(OH)_2/H_2O$ slurry exhibited pH = 8.4, which allowed adsorption of dissolved Ni^{2+} cations onto negatively charged surface of sulfided and partially re-oxidized Mo/Al_2O_3 catalysts. This reaction proceeded in ambient atmosphere for 1-8 days, depending on the temperature. The relatively high pH observed during impregnation could also cause additional increase of partial re-oxidation of surface sulfidic species to form $S_xO_y^{n-}$ [79], which was accompanied with a decrease of PZC of sulfided Mo/Al_2O_3. In principle, this partial re-oxidation reaction was beneficial for the sorption of the Ni^{2+} species.

2.4. Chelating Agent Assisted Spreading – co-deposition of Co(Ni)Mo

Both the conventional or slurry impregnation described above need deposition of Mo in the first step, which is followed by deposition of Co or Ni in the second step. The conventional precursors ammonium heptamolybdate and cobalt nitrate, moreover, normally precipitate in aqueous solutions to form cobalt molybdates. The calcination at temperature above 350 °C [80] is needed after Mo deposition from $(NH_4)_6Mo_7O_{24}$ to decompose the Mo salt prior to Co (Ni) deposition (Table 1). The ammonium and nitrate salts or oxide and hydroxide carbonate precursors were also replaced by thiomolybdates or acetylacetonates in the reports [81,82] or our work [O22] for the subsequent impregnation, respectively. Alternatively, the bimetallic Co(Ni)Mo phase is deposited in single impregnation step. This group of preparation methods includes direct dosage of the highly soluble Co(Ni)Mo precursors during the sol-gel synthesis of support [83,84], addition of chelating agents such as citric acid [85,86], nitrilotriacetic acid (NTA) [87], ethylenediamine tetraacetic acid [88], thioglycolic acid [8] to Co(Ni)Mo solutions or using heteropoly oxoanions of Keggin and Anderson types [9-12, 89].

The addition of chelating agents [87,90-104] such as of nitrilotriacetic acid (NTA) or diethylenediaminetetraacetic acid (EDTA) into the impregnating solution often resulted in increased HDS activity. Explanation in the literature is the following. A complex of a chelating agent with Co or Ni is formed. This stabilizes Co or Ni against sulfidation so that they are sulfided after Mo. The result is larger number of Co and Ni atoms decorating MoS_2 crystals, which is important for activity promotion. In the absence of chelating agent, Co and Ni are sulfided before Mo and this leads to formation of inactive bulk Co and Ni sulfides

[87,90-93]. However, the phenomenon was observed also for silica supported Co catalyst for Fischer Tropsch synthesis, where sulfidation is not involved. Thus, alternative explanation comes into account. Complex formation influences the interaction of metal species with the support and results in increased dispersion of metal compound after calcination [94,95]. The phenomenon has already been described for CoMo and NiMo supported on pure active carbon [95,96], alumina [97-103], silica [87,90,104], modified γ-Al_2O_3 [105], and wide-pore mixed ZrO_2-TiO_2 [106].

Nevertheless, the literature method of the preparation of the impregnating solution containing a chelating agent is rather complicated. The chelating agent is usually dissolved in NH_4OH, the solid MoO_3 is added and the mixture is heated until all MoO_3 dissolves. In the end, Co(Ni) nitrate is added and dissolved [87]. Alternatively, the impregnation solution is made from ammonium heptamolybdate, cobalt nitrate and NTA [101,107,108].

In contrast, we have developed a possibility of employing the chelating properties of NTA to form impregnation solution from MoO_3 and $CoCO_3$ or $NiCO_3$. The chelating properties of NTA were so strong that they allowed the dissolution of MoO_3 (solubility in water is only 1.2 g per 100 ml at 60 °C [78]) and, surprisingly, also the dissolution of the mixture of MoO_3 and $CoCO_3$. The presence of NTA in the impregnation solutions also prevents precipitation reaction. The impregnation method was named in analogy to SAS as chelating agent assisted spreading. The method appeared convenient to deposit the Co(Ni)Mo onto support in single impregnation step. Another advantage of this method was that addition of NH_4OH was not needed. Ammonia forms ammonium sulfide during in-situ sulfidation, which leads to plugging of the reaction apparatus if the reactor exit is not sufficiently heated. The activation by reduction sulfidation thus could, with advantage, be done directly after drying. [O18, O20, O22, O24]

2.5. The precursors and their reactivity in SAS

The precursors of Co(Ni)Mo that are used for SAS represent benchtop chemicals provided by Sigma-Aldrich, Merck, or AlfaAesar vendors. Nevertheless, they were activated before SAS by milling. [O6, O8, O10, O11, O17] The milling increased the surface area of the precursors and thus the rate of dissolution. To quantify these aspects, they were characterized by X-ray diffraction and nitrogen physisorption to determine their surface area (the experimental details of XRD and N_2 physisorption are described below). The solubility (S) of MoO_3 based mixtures in water and the rate of dissolution of MoO_3 in water was considered by chemical analysis by atomic absorption spectroscopy (AAS) and by conductivity measurements.

The crystal size diameter *d(XRD)* was calculated by Sherrer´s equation averaging diameters associated to the 2 theta angles 12.8, 23.3, 25.7, and 27.3 ° for MoO_3; 22.05, 36.45, and 43.03 ° for Co_3O_4; 22.09, 43.05, 36.49 ° for $Co(OH)_2$; 28.95, 37.89, and 63.17 ° for $CoCO_3.xH_2O$; 29.05, 37.99, and 63.33 ° for $CoCO_3.Co(OH)_2$. The surface area S_{NE} was determined by N_2 adsorption by Nelsen and Eggertsen flow method and the mean value of the equivalent spherical particle diameter $d(S_{NE})$ was calculated using density of MoO_3 of 2.7 g cm^{-3}. The results of the measurements of MoO_3/H_2O slurry conductivity C were correlated with the first order equation $C = PS * (1 - \exp(- k_{dis}*t))$, where PS is pseudosolubility, k_{dis} is the rate constant of MoO_3 dissolution and t is time. The values PS and k_{dis} were normalized to the most coarse MoO_3 sample (the sample of MoO_3 with the lowest dissolution rate) and they were labeled PS_{rel} and $k_{rel\text{-}dis}$. Table 2 summarizes the calculated values along with determined PZCs. Furthermore, Fig. 1 illustrates how various MoO_3 samples spread over the extrudates of aluminas with diameters 1.6 and 3.2 mm, surface area S_{BET} 262 and 217 m^2g^{-1}, pore volumes V_{Total} 0.60 and 0.76 cm^3g^{-1}, and average pore diameter D_{BJH} 8.2 and 12.1 nm, respectively.

It was found that as-received chemicals MoO_3(d), presumably prepared by thermal decomposition of $(NH_4)_6Mo_7O_{24}$, and MoO_3(s), supplied as a grade ´sublimated´, were most coarse within the MoO_3 studied. Though MoO_3(s) exhibited the lowest rate of dissolution, highest *d(XRD)* and $d(S_{NE})$, and the slowest rate of spreading over of aluminas (Fig. 1), its experimentally determined solubility *S*, by AAS, was somewhat higher than that of MoO_3(d) (Table 2). Despite that, *S* of both were similar to the tabulated values of solubility. Activation of MoO_3(d) in an agate mortar and pestle mill for 4 h, giving the sample MoO_3(d,a), did not change significantly *d(XRD)*, $d(S_{NE})$, or *S*. MoO_3(d,a) spread over the aluminas faster than MoO_3(s). Nonetheless, significant and beneficial increase of all parameters were observed after grinding of both MoO_3(d) and MoO_3(s) in planetary mill for 27 h, giving the samples MoO_3(d,p) and MoO_3(s,p).

It should be also noted that the liquid after deposition of MoO_3 over alumina, despite being colorless, usually contains about 0.5-4.4 g dm^{-3} of MoO_3, which is less than experimentally achieved solubility of MoO_3(d,p) 7.0 g dm^{-3}. The liquid also contains about 2.5 g dm^{-3} of dissolved alumina. For some aluminas, for example for that of diameter 1.6 mm (the section here), the content of MoO_3 and Al_2O_3 in the liquid was 18 and 4.8 g dm^{-3}, respectively, i.e. higher than it usually is and higher than the tabulated value is. The explanation could be found in the reaction of dissolved MoO_3 with dissolved alumina species to form $[Al(OH)_6Mo_6O_{18}]^{3-}$ anions. This reaction was described for conventional impregnation by Carrier et al. [109-111] and it seems likely that such anions are formed during SAS. Impurities specific for each alumina, such as Na or Ca, are other factor to consider. Last but not least, naturally colloidal character of part of dissolved MoO_3 activated in planetary mill may also explain higher content of Mo in experimentally prepared solution in comparison to tabulated values. In brief, specific interaction of Co(Ni) with supported MoO_3 catalysts during the promoters deposition by SAS should also be taken into account though they have not been yet quantified experimentally since the promoter content is low. Nevertheless, Co(Ni) deposition onto presulfided supported Mo catalysts naturally prevents formation of Co(Ni) polyoxomolybdates (Section 2.3 above).

In conclusion, the use of planetary mill for activation of the precursors for SAS represents important progress as regards the time of impregnation.

Table 2: Properties of different Mo and Co precursors: crystal size diameter from X-ray diffraction *d(XRD)*, surface area from N_2 physisorption S_{NE}, $m^2g^{-1}$and equivalent spherical particle size diameter $d(S_{NE})$, relative constant of the rate of dissolution $k_{rel\text{-}dis}$ and pseudo-solubility PS_{rel} from conductivity measurements, the solubility *S* from AAS, and PZC by simplified mass titration method.

Precursor	Activation	*d(XRD)* nm	S_{NE} m^2g^{-1}	$d(S_{NE})$ nm	$k_{rel\text{-}dis}$	PS_{rel}	S^a g dm^{-3}	PZC
MoO_3(d)	as received	38	1.5	851	3.7	1.1	1.3	2.5
MoO_3(d,a)	agate mortar mill 4 h	35	2.2	580	5.0	1.2	1.5	2.5
MoO_3(d,p)	planetary mill 27 h	18	17.0	75	13.6	3.2	7.0	2.5
MoO_3(s) (´sublimated´)	as received	45	0.6	2130	1.0	1.0	1.6	2.5
MoO_3(s,p)	planetary mill 27 h	20	16.8	76	16.7	2.3	7.0	2.5
Co_3O_4 (´nanopowder´)	as received	13	40	-	-	-	-	3.8
$Co(OH)_2$	planetary mill 27 h	6	90	-	-	-	-	6.7
$CoCO_3.xH_2O$	planetary mill 27 h	6	68	-	-	-	-	8.6
$CoCO_3.Co(OH)_2$	planetary mill 27 h	9	45	-	-	-	-	8.5
NiO (´nanopowder´)	as received	-	-		-	-	-	7.6
$Ni(OH)_2$	planetary mill 27 h	-	-	-	-	-	-	8.9
$NiCO_3.2Ni(OH)_2.xH_2O$	planetary mill 27 h	-	47		-		-	8.4
$2NiCO_3.3Ni(OH)_2.4H_2O$	planetary mill 27 h	-	-	-	-	-	-	10.1

[a] Tabulated solubility of MoO_3 is 0.5 g dm^{-3} and of H_2MoO_4 is 1.3 g dm^{-3}, ref. [78].

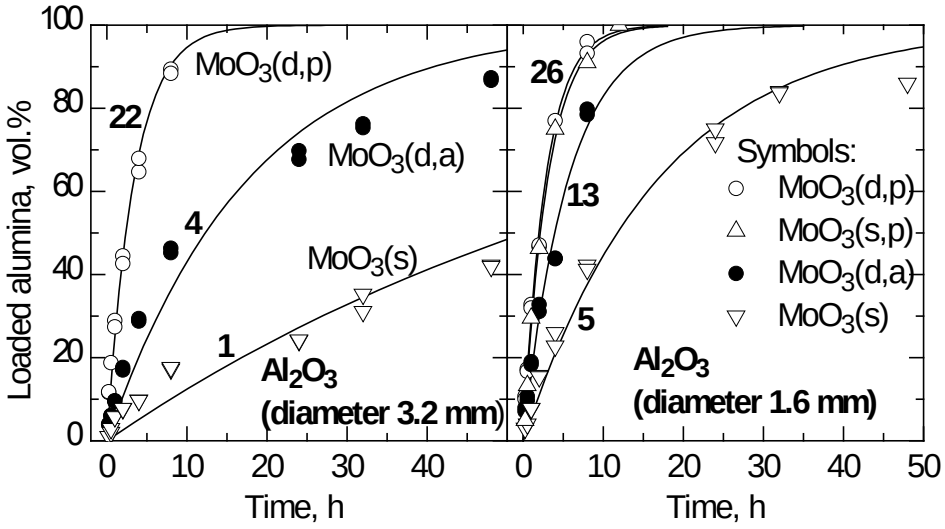

Fig. 1: Gradual saturation of the Al_2O_3 extrudates volume by adsorption of different sorts of MoO_3. The numbers represent $k_{rel\text{-}imp}$s, which were normalized per k_{imp} of MoO_3(s) determined on Al_2O_3 with the diameter 3.2 mm (the sample with the slowest rate of impregnation). The k_{imp} is the first-order rate constant of impregnation calculated from the fitting of the loaded volume LV in time t: $LV = 100 * (1- \exp (- k_{imp}*t))$. [O6]

3. Catalysts characterization

3.1. Structural characterization

The X-ray diffraction (XRD) was done to determine amount of crystalline MoO_3 phase during reaction of MoO_3 with α-AlOOH or organized mesoporous alumina (OMA) and crystalline structure of Al_2O_3 [O5, O11, O14], TiO_2 [O15], ZrO_2 [O12, O18] or C [O23, 5] based supports. It should be mentioned that crystalline phase of MoO_3 is not detected in well dispersed catalysts, which is a typical feature of catalysts prepared by SAS. [O1, O4, O5, O10-O12, O18, O19, O22]

Raman spectroscopy was also employed as a sensitive method of determination of crystalline phase MoO_3 and oxygen containing Mo species in Mo catalysts. It was found to be usefull for monitoring of re-oxidation of sulfided Mo catalysts before depostion of Ni by SAS. In Pt/C electrocatalysts synthesis [O23, 5,6], the size of turbostratic graphite crystallites, *d(G,Raman)*, were approximated from the G and D band intensity ratio [112].

Mechanical mixture homogenized in mortar and pestle was analyzed by scanning electron probe micro-analysis (SEM-EDX) for chemical analysis. The bisected catalyst extrudates were analyzed by SEM-EDX to determine radial eggshell concetration profiles of Mo or to monitor deposition of Co and Ni promoter by SAS.

The textural properties of the supports and catalysts were investigated with a static (volumetric) Micromeritics ASAP 2010 apparatus or dynamic (single point) Micromeritics FlowSorp III apparatus by N_2 physisorption. To calculate the specific surface area (S_{BET}), the data were treated by the standard BET method. Total volume of pores V_{Total} was determined from the amount of N_2 adsorbed at $p/p_0 = 0.98$. Surface area of mesopores (S_M) and volume of micropores (V_{micro}) were calculated from t–plot method modified by Schneider [113]. The pore-size distribution was calculated from the desorption branch of the adsorption isotherms by BJH method and the diameter at the maximum at pore-size distribution curve was read down and indexed as D_{BJH}. The dynamic measurements were evaluated by the method of Nelsen and Eggertsen [114] to determine surface area S_{NE}.

3.2. Chemical characterization

The point of zero charge (PZC) of the supports and catalysts was approximated by the pH of their slurries in water in the present work. This is a simplified version of the mass titration method. [115,116] The PZC of the slurry of two solids is a linear combination of their PZC multiplied by the fractions of their surface areas (for instance see Ref. [115]). Similarly, the PZC of the slurry of a supported oxide is a linear combination of the PZC of the support and the deposited oxide multiplied by the fractions of free support surface and surface covered by the deposited oxide. Such an approach was used in the literature for instance for the determination of surface coverage in the MoO_3/Al_2O_3[117], WO_3/Al_2O_3[118] or V_2O_5/Al_2O_3[119] catalysts by measuring their PZC.

Moreover, the PZC of selected samples was also obtained from a plot of zeta potential versus pH. These PZCs were conluded to be considerably similar to those PZCs achieved by the simplified mass titration method [O16,O21].

The temperature programmed reduction (TPR) was used to characterize the deposited species in their oxidic or sulfidic stage using a Miromeritics chemisorber AutoChem 2950 HP or home-made apparatus. TPR confirmed that the quality of the deposited species by SAS is similar to those deposited by conventional impregnation for the matter of comparison. [O4, O9, O12, O22]

The number of unsaturated sites in sulfided Mo and CoMo catalysts was determined by pulse O_2 chemisorption [120]. Typically, no tight correlation was observed among chemisorbed oxygen, reduction temperature in TPR, hydrogen consumption in TPR or activity in HDS reactions, which points on the presence on more than one type of catalytically active sites in the studied catalysts. [O18, O19, O22] For this reason, weight normalized activities are mostly used in the author´s works as the most sensitive technique of catalyst characterization.

The Pt dispersion in reduced catalysts was measured by H_2 chemisorption and it was expressed as the molar ratio *H/Pt* or the surface area of the metallic platinum, $S(Pt,H_2)$. It was assumed that the Pt:H chemisorption stoichiometry was 1:1 and that the number of surface atoms per unit area was $1.25 * 10^{19}$ at. m^{-2} as it was reported in literature [121,122]. The diameter of the platinum particles, $d(Pt,H_2)$, was calculated assuming spherical geometry and uniform particle size. This H_2 chemisorption was found particularly useful in prepration of Pt/C electrocatalysts. [O23]

4. Catalytic activity and selectivity

4.1. Model reactions

The activity of catalysts was studied in hydrodesulfurization (HDS) of thiophene (TH) at atmospheric pressure or 1 MPa, HDS of benzothiophene (BT) at 1.6 MPa, and parallel HDS of thiophene (TH) and HDN of pyridine (PY). The catalytic activity in the isomerization of cyclohexene (CH) and cumene (CU) cracking was taken as simple indexes of Brönsted acidity of the studied samples [123,124]. The schemes of the model hydrotreating reactions and reactions of the acidity measurements are shown in Fig. 2. The reactions were measured in laboratory tube continuous flow micro reactors. The catalyst (particle size fraction of 0.16–0.32 mm) was typically activated by sulfidation in-situ by a H_2S/H_2 mixture (1:10) at atmospheric pressure. The rate constant of the starting compound conversion or final product formation were calculated using an empirical pseudo-first-order rate equations. An example how relative composition depends on space time W/F_{BT} and how k_{EB} was obtained by the fitting of the experimental data is given in Fig. 3.

Hydrorefining:

Hydrodesulfurization (HDS)

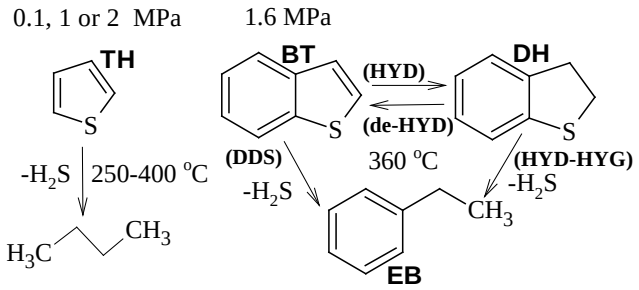

Hydrodenitrogenation (HDN)

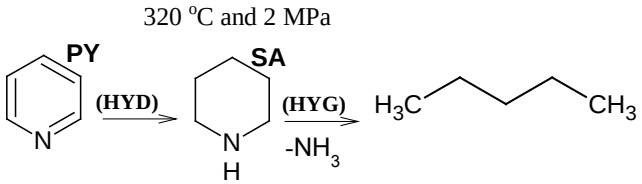

Acidity:

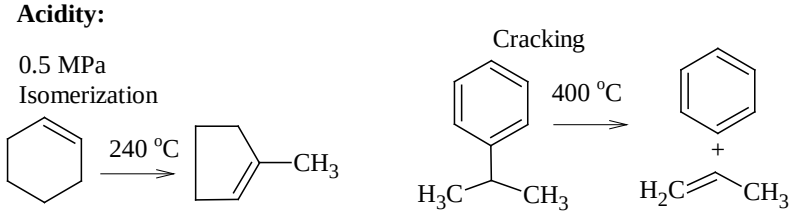

Fig. 2: Schematic overview of the model reactions applied for characterization of the prepared catalysts. HDS of 1-benzothiophene (BT): (HYD) hydrogenation of benzothiophene to dihydrobenzothiophene, (de-HYD) dehydrogenation of dihydrobenzothiophene to 1-benzothiophene, (HYD-HYG) hydrogenolysis of dihydrobenzothiophene to ethylbenzene (hydrogenation route), (DDS) hydrogenolysis of 1-benzothiophene to ethylbenzene (direct desulfurization route); HDN of pyridine (PY): (HYD) hydrogenation of pyridine to piperidine (saturated amines, SA), and (HYG) hydrogenolysis of piperidine (saturated amines, SA) to pentanes (intrinsic HDN).

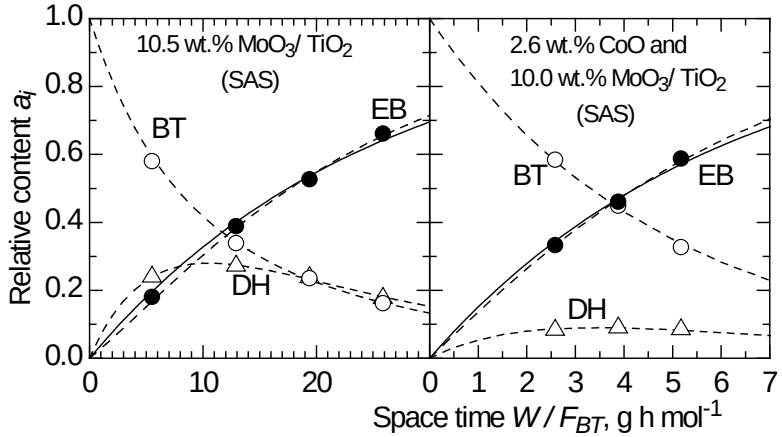

Fig. 3: Relative composition during reaction of 1-benzothiophene (BT, open circles) hydrodesulfurization over catalysts prepared on TiO_2 of S_{BET} = 140 m^2g^{-1}, V_{total} = 0.33 cm^3g^{-1} and D_{BJH} 10 nm [O16]: (DH, open triangles) dihydrobenzothiophene, (EB, solid circles) ethylbenzene, (dash lines) the curves calculated using the parallel consecutive scheme of four pseudo-first-order rate reaction from Fig. 2, (solid line) the curve calculated using an empirical pseudo-first-order rate equation to determine total HDS activity k_{EB}.

4.2. Promotion or synergism in activity and selectivity

The nature of the support (support effect), the composition of the active phase, and the method of preparation often significantly influence activity or selectivity of catalysts. Synergistic effect in the bimetallic sulfide catalysts Co–Mo, Ni–Mo and Ni–W is an important phenomenon in hydrotreating catalysis over sulfides [73]. Its magnitude is expressed as the ratio of activity of the bimetallic catalyst to the sum of activities of corresponding monometallic catalysts. This phenomenon is sometimes evaluated also in terms of promotion. The magnitude of promotion is expressed as the ratio of the activity of a bimetallic catalyst to the activity of a molybdenum catalyst.

The magnitude of promotion or synergism reported in the literature varies in a rather broad range and discussion of the literature does not fit the scope of this work. A short overview for the HDS reactions and support effect could be found in ref. [O9]. In order to illustrate the issue, the supports Al_2O_3 (S_{BET} = 262 m^2g^{-1}), ZrO_2 (S_{BET} = 108 m^2g^{-1}), TiO_2 (S_{BET} = 140 m^2g^{-1}), and SiO_2 (S_{BET} = 289 m^2g^{-1}) were impregnated by conventional impregnation using $(NH_4)_6Mo_7O_{24}$ and $Co(NO_3)_2$ to get loadings of 4 Mo nm^{-2} or 4 Co nm^{-2} or varieties of Co/Mo ratios (Fig. 4) in resultant catalysts. The activated carbon (S_M = 289 m^2g^{-1}) and MgO (S_{BET} = 300 m^2g^{-1}) supports were impregnated differently by SAS and by avoiding calcination of nitrates as it is discussed specifically for each support below in the sections 7 and 6, respectively. The synergism in activity in HDS of BT is summarized in Table 3 and Fig. 4A. The synergism in selectivity is shown in Fig. 4B.

It was clearly found that the order of activity in BT HDS (360 °C, 1.6 MPa) of monometallic Mo catalysts was MoO_3/TiO_2 > MoO_3/C > MoO_3/ZrO_2 > MoO_3/SiO_2 > MoO_3/Al_2O_3 > MoO_3/MgO, which correlated with the degree of reduction in TPR (not shown, see [O9]). The magnitude of promotion by Co in the hydrodesulfurization activity decreased in the order CoMo/MgO > CoMo/C > $CoMo/Al_2O_3$ > $CoMo/ZrO_2$ > $CoMo/TiO_2$ > $CoMo/SiO_2$. The synergism and promotion in the hydrogenolysis activity is higher than in hydrogenation and it is thus accompanied by characteristic decrease of the hydrogenation/hydrogenolysis selectivity (HYD-HYG/DDS). The synergism in DDS selectivity is manifested by a decrease of selectivity to DH in Fig. 4B. It should be mentioned that our study into HYD-HYG/DDS selectivity of the benzothiophene reaction give in principle results similar to those of studies with dibenzothiophene [125-128], where an increase in total HDS activity by promotion is accompanied by much greater increase in the direct desulfurization (DDS) reactivity pathway than in the HYD reactivity pathway. In contrast, the HYD pathway seems to be essential in the case of the recalcitrant 4,6-dimethyl-dibenzothiophene HDS. [126-129]

Table 3: Promotion and synergism in activity of catalysts in benzothiophene HDS [O9]

Support	Activity A [a], $mol_{BT}\ h^{-1}\ mol_{Me}^{-1}$ [b]			Synergism	Promotion
	Mo	Co	CoMo[c]	$A_{CoMo}/(A_{Co}+A_{Mo})$	A_{CoMo}/A_{Mo}
MgO	50	25	893	11.9	17.9
C	90	179	794	3.0	8.8
Al_2O_3	53	33	400	4.7	7.5
TiO_2	96	52	270	1.8	2.8
ZrO_2	90	29	222	1.9	2.5
SiO_2	59	31	128	1.4	2.2

[a] F_{BT}/W needed for $y_{EB}=a_{EB}=0.4$ in $mol_{BT}\ h^{-1}\ mol_{Me}^{-1}$

[b] $mol_{Me} = mol_{Mo} + mol_{Co}$ (Mo and Co at 4 atoms per nm^2, CoMo see Fig. 4 and text)

[c] catalyst with highest activity (catalyst with optimal Co/Mo ratio, see Fig. 4)

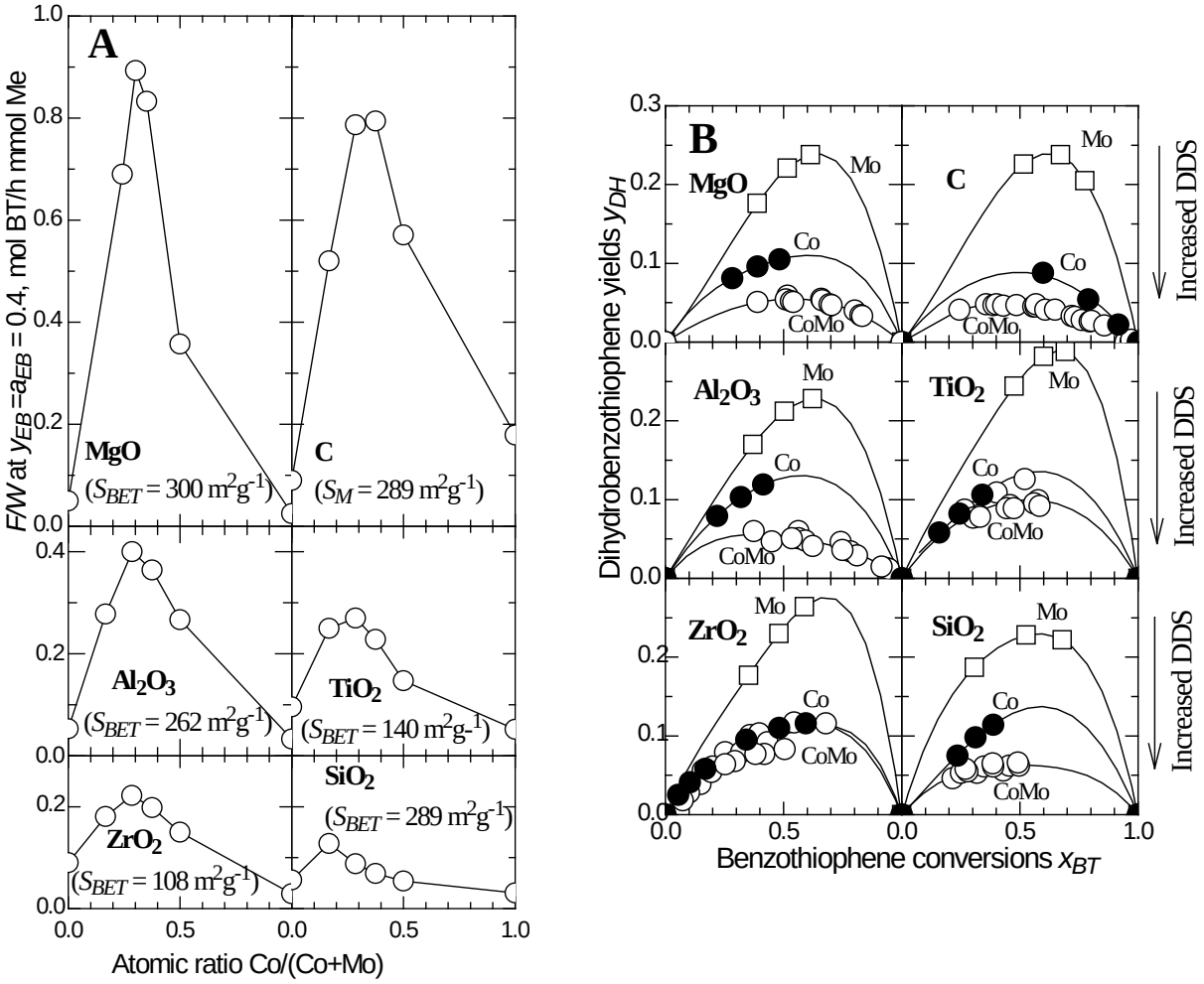

Fig. 4: The dependence of the activity of CoMo catalysts on the Co/(Co+Mo) ratio and support (**A**) and synergism in relative selectivity HYG-HYD/DDS (selectivity to dihydrobenzothiophene during benzothiophene HDS (**B**). [O9]

To demonstrate the effect of chelating agent assisted spreading, the supports Al_2O_3 (S_{BET} = 262 m^{2}g^{-1}), ZrO_2 (S_{BET} = 108 m^{2}g^{-1}), and active carbon (S_M = 289 m^{2}g^{-1}) were impregnated using MoO_3, $CoCO_3$ and NTA solutions of molar ratio NTA: (Co+Mo) = 1 and the loading 3.5 Mo nm^{-2} by the modified SAS and by conventional impregnation and the catalysts were compared in HDS of TH and BT. It was well documented that employing the chelating agent nitrilotriacetic acid in the preparation of the CoMo catalysts supported on gamma-Al_2O_3, activated carbon, and monoclinic-ZrO_2 systematically increased the promotion effect of Co in hydrodesulfurization reaction of thiophene and benzothiophene at high pressure by the factor 1.13-1.58. [O20]

It was concluded that the above mention tests of activity and selectivity represent a convenient methodology for evaluation of the catalysts novelly prepared by SAS method. Particularly the evaluation of synergy in selectivity apart from the activity is a sensitive approach that was utilized in the present work.

5. HDS catalysts supported on amphoteric oxides

5.1. Alumina

Due to its vide variety of catalytic and non-catalytic applications, Al_2O_3 provided excellent opportunity for exploration of the concept of solvent-assisted spreading. The selection of Al_2O_3 supports covered broad range of S_{BET}s from 11 to 279 m^{2}g^{-1}. This set of

aluminas with S_{BET}s of 11, 53, 77, 78, 103, 114, 127, 129, 158, 182, 206, 212, 253, 262, and 279 m^2g^{-1}, respectively, was thus allowed reacting with a surplus of MoO_3/H_2O slurry to determine saturated adsorption loading L_a on the alumina surface. The L_a corresponds to filled Mo monolayer. The quality of the deposited monolayer over various Al_2O_3 was compared by TPR [O6], and the catalytic properties were tested in thiophene HDS after deposition of promoter by SAS using $CoCO_3.Co(OH)_2/H_2O$ slurry [O10]. The catalysts were also compared to those prepared by conventional impregnation.

The dependence of L_a on S_{BET} and the saturation adsorption loading of CoO on L_a is shown in Fig. 5. The correlation of L_a, saturation adsorption loading of CoO and HDS activity is depicted in Fig. 6. It was concluded that the water-assisted spreading of MoO_3 is a simple and convenient method for preparing MoO_3/Al_2O_3 catalysts with well-developed and homogenous filled monolayer of molybdena species. The quality of monolayer evaluated by the temperature of TPR peaks was independent of alumina surface (TPR patterns are not shown, see [O4]). Water-assisted spreading of $CoCO_3.Co(OH)_2$ onto MoO_3/Al_2O_3 with the saturated monolayer of MoO_3 led to saturated loadings of Co roughly proportional to the surface of MoO_3 monolayer. This deposited Co species were effective in Mo promotion. The mean filled monolayer density determined by SAS method overt the set of 11 aluminas was 3.4 Mo nm^{-2}. The catalysts prepared by SAS are equally or more active in HDS of thiophene as compared to those prepared by conventional impregnation or reference commercial catalysts.

The determined mean filled monolayer density 3.4 Mo nm^{-2} (or 0.29 nm^2 per atom Mo) correspond well to the literature data about the saturation with $(NH_4)_6Mo_7O_{24}$ at pH 3.9 with resultant 3.1 Mo nm^{-2} [75], at pH 2 with resultant 2.4 Mo nm^{-2} [72], and about the determination of the monolayer by XPS with resultant 5.3 Mo nm^{-2} [71,130], and 4 Mo nm^{-2} [131], by XRD with resultant 5 Mo nm^{-2} [132,133] and 3.6 Mo nm^{-2} [134], or by selective CO adsorption with resultant 4.1 Mo nm^{-2} [70]. In short, the saturation by SAS gives 3.4 Mo nm^{-2}, which is higher than the values from the adsorption experiments and lower than the values from the measurements of physico-chemical properties.

The above mentioned results, however, were predominantly achieved over supports in the form of grains 0.16-0.32 mm. SAS method was also focused on shaped form of supports that are of both fundamental and practical interest. Namely, the formation of eggshell concentration profiles was explored. Previous authors prepared these catalysts using $(NH_4)_6Mo_7O_{24}$ and they concluded that lower pH, higher concentration of the solution, higher temperature during impregnation or faster drying promoted the formation of eggshell profile. [135-139] The methods of the eggshell profile evaluation included SEM-EDX, reduction with hydrazine-hydrochloric solution or gaseous hydrogen [135-139] and quite recently also UV-vis and Raman microscopy [140-145], Tomographic Energy Dispersive Diffraction Imaging [146] or Multinuclear Magnetic Resonance Imaging [147]. We have applied SEM-EDX and sulfidation with H_2S/H_2 mixture. The latter method has not been applied previously in the literature. The examples how the eggshell profiles of Mo and the profiles of Co or Ni were determined is summarized in Fig. 7 and 8, respectively.

We concluded that reaction of alumina with slurry MoO_3/H_2O is a simple and convenient method of preparation of MoO_3/Al_2O_3 catalysts with eggshell radial profile of Mo concentration. The profiles obtained are almost rectangular while the profiles obtained in the literature [135-139] are rather shallow and diffuse. The Mo concentration in the shell is practically independent of the shell thickness and is close to the filled monolayer loading. The shell thickens can be regulated by the amount of MoO_3 used. No waste solution or slurry is produced. A uniform profile is obtained when the amount of used MoO_3 corresponds to saturation adsorption loading (L_a), that is, to filled monolayer loading.

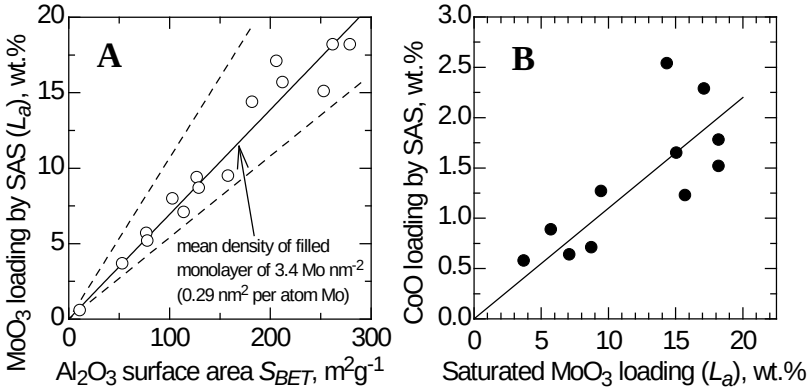

Fig. 5: The dependence of saturated amount of MoO_3 adsorbed (L_a) in SAS on alumina surface (A) [O6] and the dependence of the amount of CoO adsorbed by SAS on saturated loading of MoO_3 (L_a) in CoMo catalysts (B) [O10]; (dash lines) dash lines define the scope of the range 0.17 – 0.37 nm^2 per atom Mo determined by varieties of techniques, refs. in [O4]; (solid lines) linear correlations.

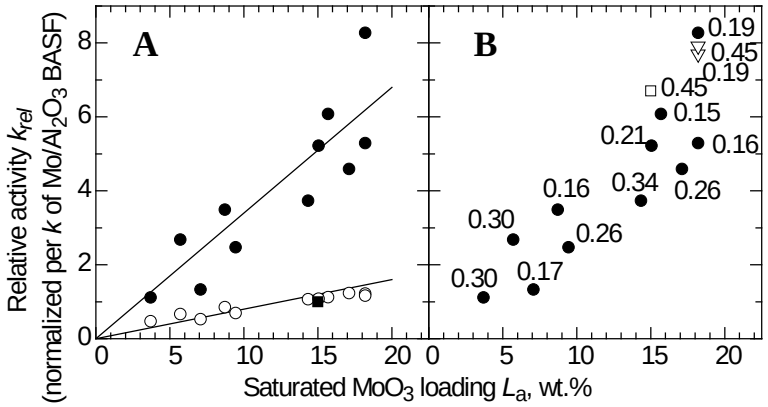

Fig. 6: The dependence of catalytic activity in HDS of TH at 310 °C and 1 MPa on L_a in Mo (open circles) and CoMo catalysts (full circles) prepared by SAS (circles) or on the Mo loading deposited by conventional impregnation for the matter of comparison (open triangle) or on the loading in reference industrial Mo (full square) and CoMo (open squares) catalysts; (**A**) the comparison of Mo and CoMo; (**B**) the points of CoMos are the same as in (**B**) but the atomic Co/Mo ration is indicated. The reference catalysts are Mo/Al_2O_3 BASF M8-30 and $CoMo/Al_2O_3$ Shell 344. [O10]

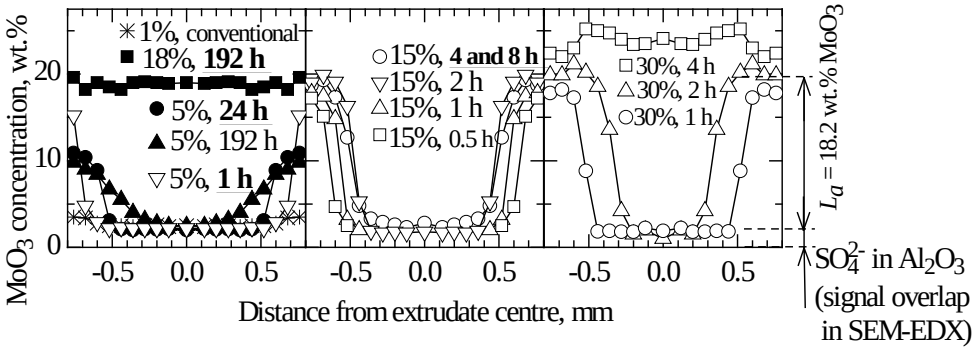

Fig 7: Reaction of MoO_3/H_2O with γ-Al_2O_3 (S_{BET} = 262 m^2g^{-1}, V_{Total} = 0.60 cm^3g^{-1}, and D_{BJH} = 8.2 nm) followed by SEM-EDX: the bold and underlined values means that all MoO_3 disappeared from the slurry at the given time; Open and filled points are for the temperatures of impregnation 100 and 25 °C, respectively. [O2]

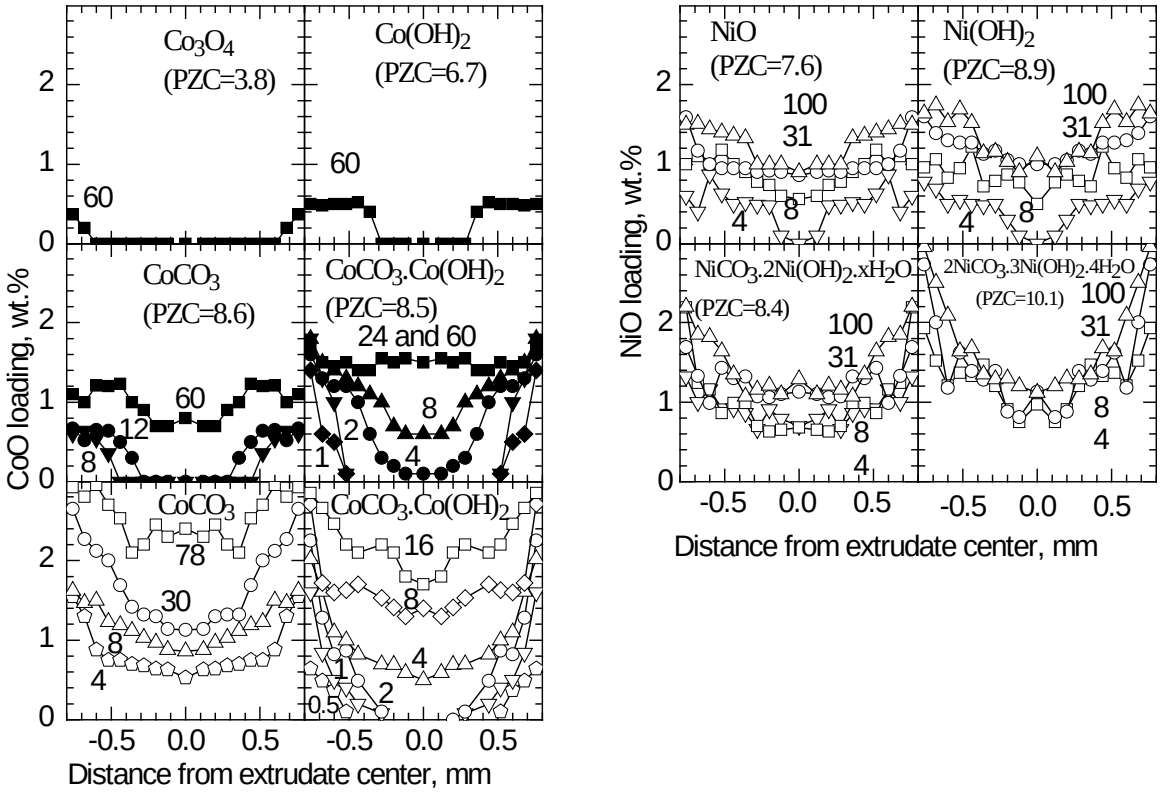

Fig. 8: CoO and NiO concentration profiles evaluated by SEM-EDX in Co(Ni)Mo/Al_2O_3 extrudates prepared by SAS onto 18.2wt.%MoO_3/Al_2O_3 catalyst. The numbers are impregnation times in hours. Open and filled points represent spreading at the temperature of 100 and 25°C, respectively. [O10, O17]

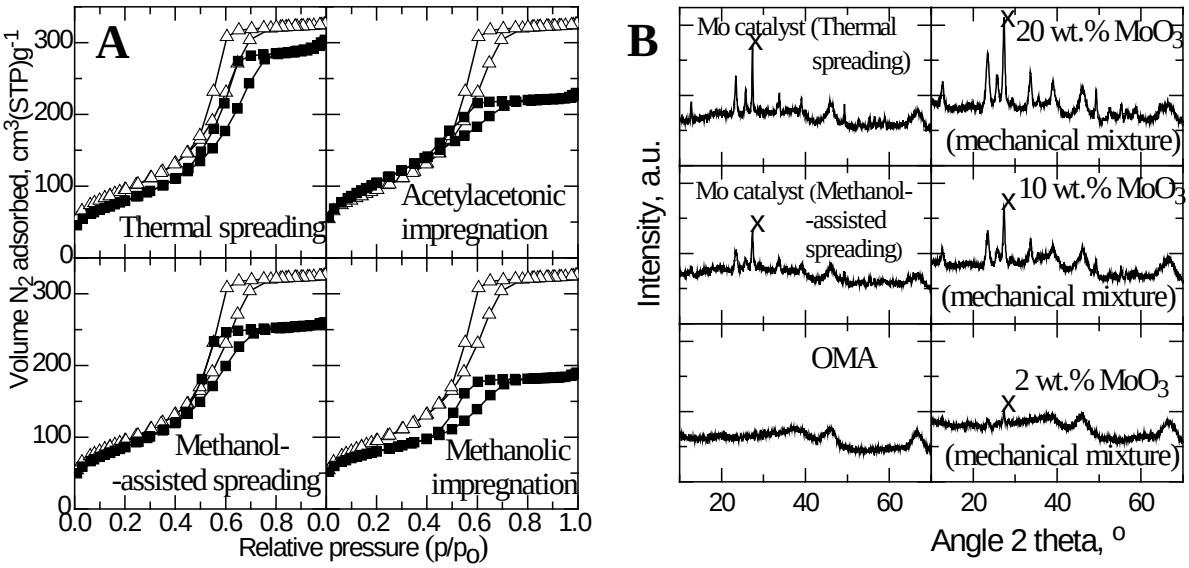

Fig. 9: Influence of Mo deposition method on N_2 adsorption–desorption isotherms of OMA (**A**) and XRD patterns (**B**). All catalysts contained 3.4 Mo nm^{-2}. Open triangles, original Al_2O_3; filled squares, Mo catalysts after HDS of benzothiophene; x, the reflection of the MoO_3, the integral intensity of which was used for the quantification of the content of the crystalline MoO_3 phase (see text). [O14]

The research into Co and Ni concentration profiles (Fig. 8) showed that SAS is a feasible method to deposit Co and Ni from aqueous slurries of $Co(OH)_2$, $CoCO_3.Co(OH)_2$,

$CoCO_3$, NiO, $Ni(OH)_2$, $NiCO_3.2Ni(OH)_2.xH_2O$, or $2NiCO_3.3Ni(OH)_2.4H_2O$ onto MoO_3/Al_2O_3 extrudates favoring the $Co(OH)_2$, $CoCO_3.Co(OH)_2$, $NiCO_3.2Ni(OH)_2.xH_2O$, or $2NiCO_3.3Ni(OH)_2.4H_2O$ precursors, i.e. precursors with high PZCs, and SAS at 100 °C. [O2, O6, O10, O17]

It has been demonstrated above that the capacity of aluminas, possessing S_{BET}s in the range 150-250 m^2g^{-1}, to disperse molybdena in the form of monolayer is about 11-17 wt.% MoO_3. The content of MoO_3 in commercial and laboratory hydrotreating catalysts falls into this range. The overloading of these aluminas with MoO_3 (independently on the method of deposition) led to constant or even decreasing hydrodesulfurization activity [148,149]. Recently, organized mesoporous alumina (OMA) has been synthesized exhibiting S_{BET}s in the range 350-700 m^2g^{-1} and relatively narrow pore sizes between 3 and 10 nm [150-153]. These textural properties thus should be able to disperse higher loading of MoO_3, which should result in an increased hydrodesulfurization activity normalized per gram of catalyst. Nevertheless, thinner walls of this high surface area Al_2O_3 in comparison to conventional aluminas naturally evoke consideration on hydrothermal stability. For this reason, the studied OMAs were impregnated i) conventionally using aqueous solution of $(NH_4)_6Mo_7O_{24}$ but the temperature of drying at vacuum evaporator was decreased to 50 °C [1,2]; ii) by thermal spreading method, i.e. spreading of MoO_3 onto OMA surface from the mechanical mixture of MoO_3 and OMA at 500 °C in air flow [1, O14]; iii) by non-aqueous conventional impregnation method with solution of molybdenyl acetylacetonate in acatylacetone or methanol [O14]; iv) and by our original methanol-assisted spreading method [O14]. Details of SAS using methanol are discussed in Section 7 dealing with MgO. The Co and Ni promoters were deposited over Mo/OMAs from ethanolic or methanolic solutions of nitrates or acetylacetonates of the metals. Nominal loadings in our experiments were 30 wt.% MoO_3 [1,2] or 26 wt.% [O14] and molar Co(Ni)/((Co(Ni)+Mo) ratio 0.3 [O14].

The results of the activity stability test in thiophene HDS did not significantly differ from the reference conventional catalyst. The relative activity index k_{rel} (k_{TH} of Mo/OMA / k_{TH} of Mo/Al_2O_3 BASF with 15wt.% MoO_3) was about 2.12 and 2.08 after 20 and 560 min on stream, respectively. [1,2] In more detailed study of OMA-supported catalysts [O14], it was confirmed that OMA exhibited significantly higher capacity for dispersion of Mo species than the conventional alumina. For example, XRD determined about 10 wt.% and 6 wt.% of MoO_3 in crystalline phase in Mo/OMA catalysts prepared by thermal spreading and methanol-assisted spreading of MoO_3, respectively, over OMA with S_{BET} = 344 m^2g^{-1}, V_{Total} = 0.67 cm^3g^{-1}, V_M = 217 m^2g^{-1}, V_{micro} = 77 mm^3g^{-1} and D_{BJH} = 4.8 nm [O14]. Nonetheless, the impregnation with methanolic solution of molybdenyl acetylacetonate verified optimal value for Mo loading at 3.4 atoms of Mo per nm^2. The adsorption-desorption isotherms, XRD patterns and activity and selectivity data in HDS of benzothiophene and simultaneous HDS/HDN of thiophene/pyridine of selected samples are summarized in Figs. 9, 10 and Table 4.

It was concluded that the methods of Mo deposition may be ranked according to the resultant HDS activity as follows: thermal spreading < methanol-assisted spreading (SAS) < acetylacetonic impregnation < methanolic impregnation. The impregnation of the high surface area of OMA from the solution of MoO_2–acetylacetonate in methanol led to highly active catalysts in HDS of benzothiophene because the organized mesoporous support, corresponding to its high surface area, was able to disperse about 1.7-fold more Mo than the support in the reference industrial catalyst. The effect of the high loading of Mo was not so pronounced in parallel HDS of thiophene with HDN of pyridine as was the case of benzothiophene HDS (Table 4).

For preparation of bimetallic Co(Ni)Mo sulfide phase, sequential impregnation from the precursor solutions in methanol with sulfidation in between was found to be, from a practical aspect, the most feasible way to deposit the conventional active metals onto this new support. The HDS activity of Mo sulfide catalysts supported on OMA was efficiently promoted by Co and Ni from solution of Co and Ni acetylacetonate in methanol. The promotional effects of Co and Ni in HDS were significantly pronounced irrespective of the presence of pyridine. The prepared CoMo catalyst exhibited more than 50% improvement of both HDS and HDN activity in comparison to the reference industrial catalyst CoMo KF 756. The prepared NiMo catalysts were about 1.3-fold more active in both HDS reactions but only about as active as the reference NiMo KF 846 catalyst in HDN.

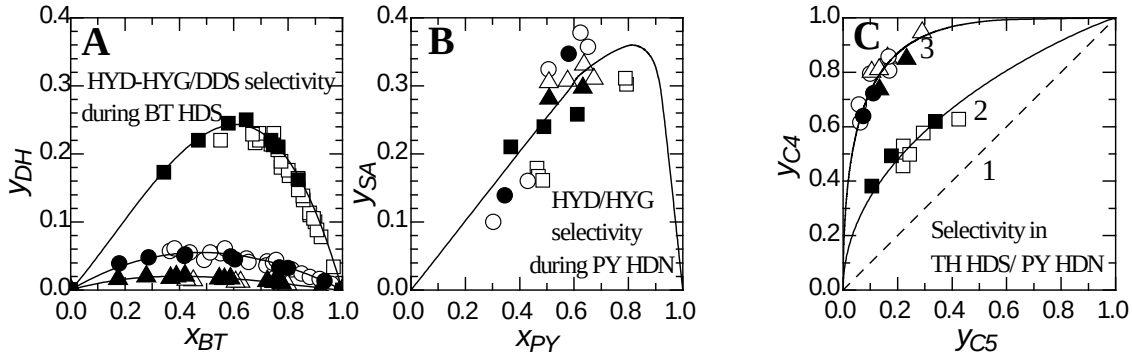

Fig. 10: Formation of dihydrobenzothiophene (DH) during HDS of benzothiophene (BT) (**A**), i.e. relative HYD-HYG/DDS selectivity in Fig. 3; formation of saturated amines (SA) during parallel HDS of thiophene and HDN of pyridine (PY) (**B**), i.e. relative HYD/HYG selectivity in Fig. 3; and selectivity HDS/HDN in parallel HDS of thiophene (y_{C4}) and HDN of pyridine (y_{C5}) (**C**) over the prepared (open symbols) and reference (filled symbols and continuous lines) catalysts. Squares, Mo catalysts; circles, CoMo catalysts; triangles, NiMo catalysts; line 1, a hypothetical catalyst with the same HDS and HDN activity; line 2, Mo catalysts (squares); line 3, promoted CoMo (circles) and NiMo (triangles) catalysts. [O14]

Table 4: Relative activities k_{rel} of the selected OMA-supported catalysts to reference industrial Mo, CoMo, and NiMo counterparts normalized per mol of Me (Intr.), unit weight (W) or volume (Vol.). [O14]

Catalyst	HDS of benzothiophene			Parallel HDS/HDN of thiophene/pyridine					
				Thiophene HDS			Pyridine HDN		
	$k_{rel\ EB}^{Intr.}$	$k_{rel\ EB}^{W}$	$k_{rel\ EB}^{Vol.}$	$k_{rel\ C4}^{Intr.}$	$k_{rel\ C4}^{W}$	$k_{rel\ EB}^{Vol.}$	$k_{rel\ C5}^{Intr.}$	$k_{rel\ C5}^{W}$	$k_{rel\ EB}^{Vol.}$
Mo^{MAS}	1.1	1.8	3.0	0.4	0.7	1.2	0.8	1.4	2.4
Mo^{MI}	1.8	2.3	5.0	0.6	0.7	1.6	1.0	1.3	2.9
$Co^{MI}Mo^{MAS}$	1.4	2.0	3.5	0.7	1.1	1.9	0.5	0.7	1.2
$Ni^{MI}Mo^{MAS}$	1.0	1.2	1.6	1.0	1.1	1.5	0.6	0.6	0.9
$Co^{MI}Mo^{MI}$	1.0	1.5	2.5	1.4	2.1	3.6	1.1	1.6	2.8
$Ni^{MI}Mo^{MI}$	1.1	1.3	1.8	1.1	1.3	1.7	0.8	0.9	1.3

[MAS] Methanol-Assisted spreading of MoO_3 onto organized mesoporous Al_2O_3 (OMA); modified SAS method

[MI] Methanolic Impregnation of i) organized mesoporous Al_2O_3 (OMA) using solution of molybdenum dioxide diacetylacetonate or of ii) sulfided Mo/Al_2O_3 (OMA) catalysts using solution of acetylacetonates of Co or Ni

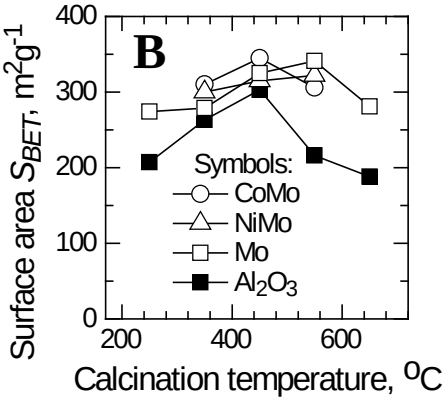

Fig. 11: The dependence of surface area S_{BET} on calcination temperature [O5, O14, O11].

Table 5: Activity of the reference catalysts and catalysts prepared in paste by SAS over α-boehmite (15 wt.% MoO_3, 3 wt. % of Co(Ni)O) in HDS of benzothiophene at 360 °C. The temperature of drying or calcination is given in brackets. [O11]

Catalyst	k_{EB}, mmol $g^{-1}h^{-1}$	Catalyst	k_{EB}, mmol $g^{-1}h^{-1}$
Mo/Al_2O_3 BASF M8-30	29		
CoMo (140 °C)	606	NiMo (140 °C)	344
CoMo (350 °C)	669	NiMo (350 °C)	308
CoMo (450 °C)	311	NiMo (450 °C)	229
CoMo (550 °C)	254	NiMo (550 °C)	161
$CoMo/Al_2O_3$ KF 746	421	$NiMo/Al_2O_3$ KF 856	434

Nonetheless, a traditional precursor of γ-Al_2O_3 supports is the α-boehmite (α-AlOOH) of various sources. During α-boehmite paste processing, the mixture of AlOOH, water, peptizing acid and/or binder is kneaded. The peptizing acid reacts with AlOOH to form low amount of binder solution. This binder solution intensifies re-agglomeration of boehmite particles, which is important in the shaping process and for the mechanical strength of final γ-Al_2O_3. Variety of peptizing acids studied could be found elsewhere [154-156]. It was also reported that Co, Ni, P and Mo can be added into α-AlOOH during paste processing and that the deposited species exhibited activity comparable to that of reference industrial catalysts [157]. Nevertheless, these syntheses in all cases involved impregnation solutions based on well soluble metal salts such as $(NH_4)_6Mo_7O_{24}$, Co and $Ni(NO_3)_2$. The purpose of our work was to explore the application SAS to α-AlOOH. Acidic conditions (pH=2.8) during reaction of MoO_3/H_2O with α-AlOOH should thus have led to partial peptizing of α-AlOOH to improve mechanical strength and/or to stabilize support texture (to inhibit sintering) during calcination. Furthermore, the effect of deposition of promoters from aqueous slurries of $CoCO_3.Co(OH)_2$ or $2NiCO_3.3Ni(OH)_2.4H_2O$ onto MoO_3/α-AlOOH was studied.

The reaction of MoO_3/H_2O with α-AlOOH was observed by XRD and the effect of calcination temperature on textural properties of the resultant catalyst was investigated by N_2 physisorption (Fig. 11). It was concluded that the reaction of α-boehmite with MoO_3 in paste followed by calcination is a simple way of preparation of MoO_3/γ-Al_2O_3 catalysts. The bimetallic CoMo and NiMo catalysts could be prepared by a sequential reaction of α-boehmite with MoO_3 and Co or Ni carbonates in an aqueous paste. Monolayer of molybdena species on α-boehmite inhibited sintering during calcination at temperatures above 450 °C (MoO_3 functioned as a textural stabilizer of Al_2O_3) despite the fact that molybdic acid did not work as a binder and did not increase the hardness of the calcined product. Activity in HDS of thiophene of the prepared Mo catalysts by SAS was about the same as activity of the

reference industrial counterpart [O5]. The deposited promoters enhanced efficiently the catalytic activity in HDS of benzothiophene. Drying at 140 and/or calcination at 350 °C of the prepared CoMo and NiMo catalysts was found to lead to the most active catalysts, the HDS activity of which was by about 1.6 times higher and 0.8 times lower than that of their commercial counterparts CoMo KF756 and NiMo KF846, respectively. However, calcination at temperatures above 350 °C decreased their HDS activity (Table 5). The selectivity in C=C hydrogenation (HYD-HYG) / C-S hydrogenolysis (DDS) over all prepared catalyst was practically the same as over the commercial CoMo and NiMo catalysts. [O11]

5.2. Zirconia

Besides conventional impregnation of zirconia, ZrO_2, or hydrous zirconia, $ZrO(OH)_2$, carriers, the MoO_3/ZrO_2 catalysts were studied in the literature using the equilibrium adsorption method [35,61,158]. Furthermore, an aqueous solution of ammonium dimolybdate instead of heptamolybdate was used in the work [53] while Mo hexacarbonyl vapors were used in ref. [42]. Nonetheless, only two alternative methods of MoO_3/ZrO_2 preparation have been published for hydrodesulfurization (HDS) catalysis: Pizzio et al. [159] deposited active species from an ethanol–water solution of molybdophosphoric acid, whereas Breysse and co-workers [160,161] introduced a molten salt method, in which ammonium heptamolybdate, zirconium oxychloride, sodium and potassium nitrates were heated at 400 °C. Previous studies also found that Mo species supported on zirconia were at least twice as active as those supported on alumina in the HDS of thiophene and dibenzothiophene and the references are provided in [O12, O15]. The aims of our work were to apply principles of SAS for preparation of MoO_3/ZrO_2 based HDS catalysts.

We found that MoO_3 can be spread over zirconia (S_{BET} 108 m^2g^{-1}, V_{Total} 0.26 cm^3g^{-1}, D_{BJH} 8 nm) and hydrous zirconia (S_{BET} 311 m^2g^{-1}, V_{Total} 0.17 cm^3g^{-1}, D_{BJH} 2 nm) using the aqueous slurry of the compound. The saturated adsorption of the resulting monolayers, L_a, exhibited densities of 3.2 and 3.5 Mo nm^{-2}, i.e. actual loadings 7.6 and 20.8 wt.% of MoO_3, for zirconia and hydrous zirconia, respectively. The deposited Mo species stabilized the high surface area of the originally hydrous zirconia after calcination at 450 °C as it is documented in Fig. 12. In this respect, the amorphous hydrous zirconia behaved as α-boehmite discussed above in section 5.1. The resultant HDS activity towards thiophene and BT, however, strongly depended on the crystallographic structure of the zirconia support. Only the monoclinic form of ZrO_2, baddeleyite, yielded high HDS activity of the supported Mo species; these species were about twice as active as that in alumina-supported catalysts. However, catalysts supported on amorphous hydrous zirconia were practically inactive despite their high specific surface area and high Mo loading. Furthermore, the intrinsic activity of Mo species deposited by water-assisted spreading was found to be slightly higher than that obtained through deposition by conventional impregnation with an ammonium molybdate solution.

Catalysts with saturated adsorption loading of MoO_3 supported over monoclinic ZrO_2 were successfully promoted from low-solubility Co and Ni carbonates using the principles of water-assisted spreading (SAS). The obtained CoO and NiO adsorption loadings were similar to the optimal loading needed for effective promotion of HDS activity. In addition, the catalysts exhibited higher HDS activity and better DDS/HYG-HYD selectivity than those promoted conventionally from solution of Co and Ni nitrates. Nonetheless, the highest activities were achieved by selective promotion of the supported MoS_2 slabs from ethanolic solutions of Co and Ni acetylacetonates. The bimetallic catalysts supported on zirconia resulted only in similar HDS activity and slightly lower DDS/HYG-HYD selectivity than achieved with commercial alumina-supported bimetallic catalysts.

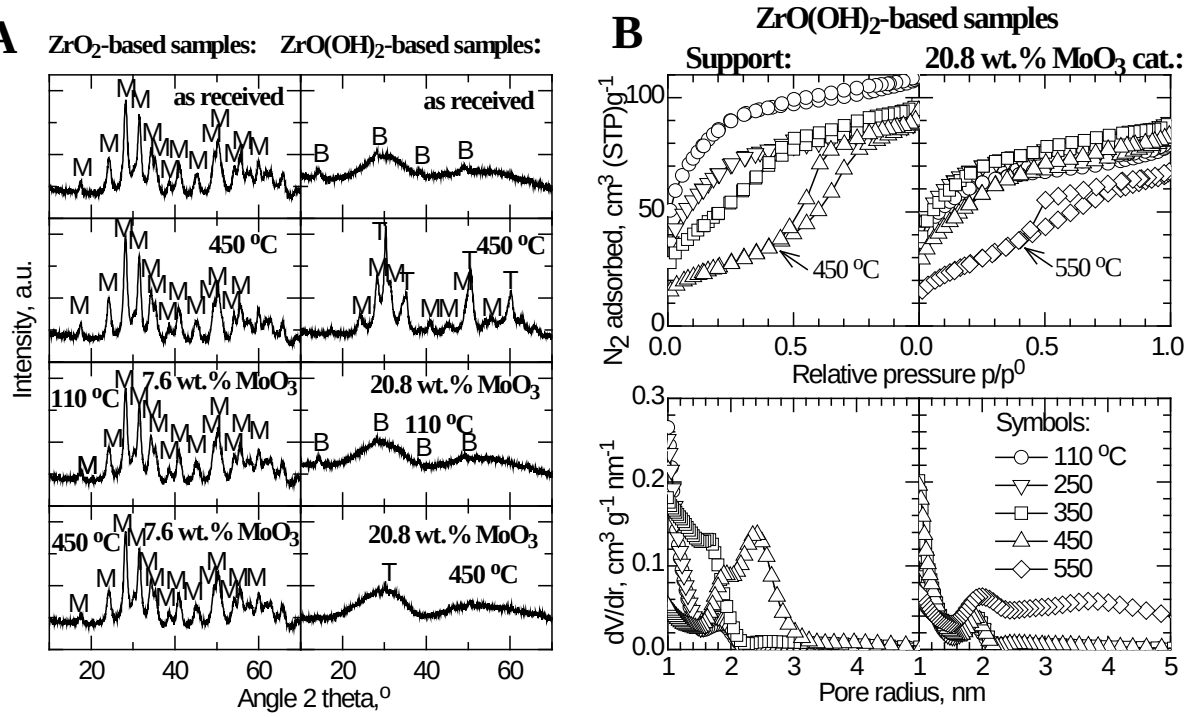

Fig. 12: XRD patterns (**A**) and the effect of temperature and Mo deposition on nitrogen adsorption isotherms and pore-size distribution of $ZrO(OH)_2$ based samples (**B**). Drying or calcination temperatures are given. M, monoclinic phase of ZrO_2; T, tetragonal phase of ZrO_2; B, α-boehmite phase of hydrous Al_2O_3 (binder in $ZrO(OH)_2$ extrudates). [O12]

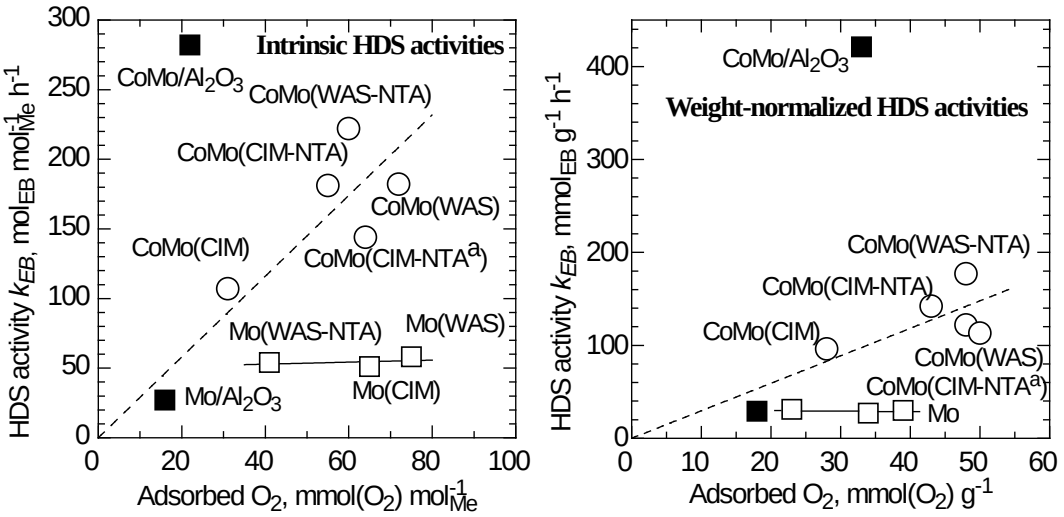

Fig. 13: The effect of preparation method on HDS activity and sulfur vacancies (O_2 up-take) of baddeleyiete supported CoMo catalysts: filled squares – reference industrial Al_2O_3 supported catalysts, open squares and solid line - ZrO_2 supported Mo catalysts, open circles and dash line – ZrO_2 supported CoMo catalysts; WAS – water assisted spreading, CIM – conventional impregnation; NTA – modification with NTA at molar ratio NTA/(Co+Mo) = 1 or NTA[a] at molar ration NTA/Co = 1.

The effect of NTA addition (chelating agent assisted spreading method) during impregnation of the monoclinic ZrO_2 on increased HDS activities [O18] was discussed above in the section 4.2. A detailed view comparing HDS actvivities and sulfur vacancies (O_2 up-take) of baddeleyite supported catalysts is in Fig. 13. The approximate linear correlation between HDS activity and amount of chemisorbed O_2 was observed for all $CoMo/ZrO_2$

catalysts. However, the point for reference industrial $CoMo/Al_2O_3$ catalyst strongly deviates from this correlation. This corresponds to experience reported in the previous literature. The reasonable correlation HDS activity – adsorbed amount of O_2 was generally observed only for a family of closely related Co(Ni)Mo catalysts [73]. From a practical view, the highest HDS activity achieved over $CoMo/ZrO_2$ catalyst prepared from MoO_3 and $CoCO_3$ and NTA by chelatin agent assisted spreading represented only about 80 % activity of the intrinsic activity of commercial $CoMo/Al_2O_3$ catalyst despite the fact that the commercial catalyst adsorbed quite low amount of O_2 (Fig. 15). Because the studied ZrO_2 exhibited only S_{BET} 108 m^2g^{-1} (i.e. only 41 % of the specific surface area of the industrial catalyst with S_{BET} 264 m^2g^{-1}), it could be expected that further improvement of catalytic activity can be achieved by increasing the surface area of the monoclinic ZrO_2. Higher specific surface area should disperse more active phase and so the HDS activity of the alumina supported catalysts would be overhelmed.

5.3. Titania

TiO_2 support is similar to ZrO_2 support in the way that the intrinsic HDS activity of Mo (activity normalized per atom of Mo) for Mo/TiO_2 is superior to that for comparable Mo/Al_2O_3 catalysts; refs. in [O7, O13, O15]. Nevertheless, surface area S_{BET} of TiO_2 supports was typically low (below 50 m^2g^{-1}) and only limited results were reported for TiO_2 with higher S_{BET}: 101 [162], 120 [163] and 160 [164] m^2g^{-1}. The aim of our work was to investigate three sets of catalysts supported over TiO_2 with high surface areas S_{BET} of 140, 230, and 407 m^2g^{-1} in HDS of thiophene or benzothiophene. Saturated adsorption loadings were determined by conventional impregnation and SAS method.

It was found that PZC of the TiO_2s of S_{BET} = 140 m^2g^{-1}, V_{Total} = 0.33 cm^3g^{-1}, V_M = 138 m^2g^{-1}, V_{micro} = 3 mm^3g^{-1}; S_{BET} = 230 m^2g^{-1}, V_{Total} = 0.48 cm^3g^{-1}, V_M = 229 m^2g^{-1}, V_{micro} = 3 mm^3g^{-1}; and S_{BET} = 407 m^2g^{-1}, V_{Total} = 0.31 cm^3g^{-1}, V_M = 371 m^2g^{-1}, V_{micro} = 21 mm^3g^{-1} was 5.0; 8.1; and 10.5; respectively. The saturated monolayer loading determined by conventional impregnation and evaluated by HDS activity and PZC measurements did not correlate with the surface area S_{BET} of the supports. The activity of catalysts supported on these tree supports increased up to loading of about 20 wt.% MoO_3 and then decreased. All MoO_3/TiO_2 catalysts with corresponding loadings were more active than a commercial sample of reference industrial 15 wt.% MoO_3/Al_2O_3 catalyst. PZC decreased with the loading for all the supports to the value for MoO_3 (2.1); however, according to this criterion, the surface of nano-TiO_2 with S_{BET} 407 m^2g^{-1} was already covered at the unexpectedly low loading of about 14 wt.% MoO_3. The extensive factor of high S_{BET} of 407 m^2g^{-1} of nano-TiO_2 of was thus not utilized as it was expected because nano-TiO_2 did not disperse a greater amount of MoO_3. [O13]

In contrast, SAS of MoO_3 on the TiO_2 with S_{BET} = 140 m^2g^{-1} (monoclinic, anatase [O15]) led to saturated adsorption monolayer loading L_a of 3.3 atoms Mo per nm^2, i.e. 10.5 wt.% of MoO_3, which was well within the range obtained above for set of Al_2O_3s (Section 5.1.). The MoO_3 concentration in the eggshell was also close to that value. The HDS activity of the active phase deposited by SAS was at least the same at of a phase deposited conventionally. [O7]

6. HDS catalysts supported on activated carbon

Activated carbons as a support of HDS catalysts [O1] differ from amphoteric oxides and mainly γ-Al_2O_3 in the following aspects: i) Mo, CoMo and NiMo sulfided catalysts exhibit better activity per unit weight than their alumina-supported counterparts; ii) Other advantages of carbon-supported catalysts include reduced coking propensity, resistance to nitrogen poisoning and easy metal recovery by burning the support; iii) High microporosity, insufficient mechanical properties and low density (since in industrial applications the activity

per unit volume is more important than the activity per unit weight) are probably the main reasons why they have not been applied industrially up to now. However, the remarkably high activity of carbon-supported sulfides is the driving force for further research.

Nevertheless, the amphoteric oxides $Me_{(1\ or\ 2)}O_{(2\ or\ 3)}$ are capable of chemical interactions (various types of OH groups, $Me^{3+\ or\ 4+}$ sites) that are large enough to achieve the formation of a monolayer of molybdena species. Pure physical adsorption (involving only Van der Waals' forces) of molybdena species does not seem to contribute significantly to the overall loading achieved by equilibrium adsorption impregnation of the 'flat' surface of non-microporous oxides. In contrast, a variety of functional groups exists on the surface of activated carbons (OH, C=O, COOH, groups, for instance [165,166]) and the details of the chemical interaction of molybdate species with carbon surfaces are not fully understood. The relation between the surface chemical properties of carbon supports on the one side and their ability to adsorb molybdenum species from solutions (in conventional equilibrium adsorption impregnation) and HDS activity of Mo/C catalysts on the other side was intensively studied in the literature but no clear correlation was observed (for instance see Refs. [167-169]).

It should be expected that the 'chemical' (or 'specific') interactions of polar functional groups with polar molybdena species are the most important driving force for the adsorption of molybdena species. However, it is not certain whether the surface density of these 'chemical' (or 'specific') sites is high enough to allow the formation of a molybdena monolayer. The 'physical' (or 'non-specific') interaction of molybdena species with a 'flat' carbon surface not containing functional groups is assumed to be weak. However, it is expected that the 'physical' sorption is strongly promoted by the closeness of opposing walls in micropores (for instance, for adsorption in slit micropores see Ref. [170]). The volume filling of micropores (leading to 'multilayer' structures) probably contributes significantly to the overall molybdena sorption in the present slurry impregnation (SAS) method.

The PZC of the activated carbons used in the present work was 8.2, 10.2, 7.2 and 8.2 for the supports Norit RX (S_{BET} = 1190 m^2g^{-1}, S_M = 454 m^2g^{-1}, V_{micro} = 390 mm^3g^{-1}), Norit RO (S_{BET} = 850 m^2g^{-1}, S_M = 201 m^2g^{-1}, V_{micro} = 330 mm^3g^{-1}), GA-05 (S_{BET} = 1053 m^2g^{-1}, S_M = 225 m^2g^{-1}, V_{micro} = 420 mm^3g^{-1}) and Chezacarb (S_{BET} = 791 m^2g^{-1}, S_M = 488 m^2g^{-1}, V_{micro} = 230 mm^3g^{-1}), respectively. The low natural pH of the impregnation slurry MoO_3/water of about 2.9 was below these PZC values and this was advantageous for the adsorption of molybdate anions. For example, the pH of the slurry containing 40 wt.% MoO_3+60 wt.% C (GA-05) at room temperature gradually decreased from an initial value of about 6 to a value of about 2.7 after 24 h as the fraction of molybdena surface area in the slurry increased by adsorption. The pH of the slurry asymptotically approached the value of about 2.3 during an additional period of 10 days. At an increased temperature of about 100°C the adsorption process and the decrease of the pH were much faster, and the pH value of about 2.3 was reached already after 1.5 h.

Furthermore, the dried Norit-RX-supported MoO_3 catalysts with various loading of the compounds were slurried in a small amount of water and their pH was measured. The pH decreased with actual loading from 8.2 for the pure support to about 2.5 for a loading of 15 wt.% MoO_3, and remained at about 2.4–2.6 for higher loadings up to the saturation adsorption loading of 33wt.%. It is noted that the fraction of the support surface available for 'chemical' ('specific') interactions is important for PZC determination and that this fraction was covered by molybdena species at a loading of about 15 wt.% MoO_3. The 'chemically' bound molybdena has mostly the character of 'monolayer' structures and influences the surface properties of the supported catalysts (PZC in the present case). Further sorption between about 15 and 33 wt.% probably occurred by 'physical' ('non-specific') adsorption. This 'physically' bound molybdena has mostly the character of 'multilayer' structures and does not influence the surface properties directly. This idea is supported by activity data as discussed

henceforward. It is also compatible with the significant drop of V_{micro} near saturation as shown in Fig. 14A.

The PZC of the other saturated carbon-supported catalysts were also close to the PZC of MoO_3 (2.9, 2.7 and 2.6 for Norit RO, GA-05 and Chezacarb, respectively), thereby confirming that the chemical sites at the support surface are completely covered by molybdena species in the saturated samples.

Using low solubility Co carbonates, SAS over the carbon supports alone and over the catalysts with MoO_3 loading lower than 15 wt.% of MoO_3 could not be achieved. This is attributed to both the small difference in PZC between these solids and the impregnation compound, and by the low solubility of the impregnation compound. The impregnation of the saturated MoO_3/C(Norit RX) catalyst with 33 wt.% MoO_3 was more successful. Cobalt probably adsorbs in the form of a cation and the point of zero charge of the saturated MoO_3/C catalyst 2.6 was well below the pH of the impregnation slurry of about 8–9. However, the maximum amount of CoO deposited was rather small and only the catalysts with 2-3 wt.% of CoO were prepared. In the attempts to prepare the catalysts containing 5 wt.% CoO by SAS, the powder of Co hydroxide carbonate did not disappear from the slurry.

It was concluded that the capacity of activated carbons for MoO_3 adsorption is very high, with saturated loadings of 27–34 wt.% MoO_3 having been achieved. Up to a loading of about 15 wt.% on a typical activated carbon (Norit RX), molybdena species are mostly adsorbed by chemical interactions with the surface in a 'monolayer' form that influences surface properties such as point of zero charge or catalytic activity (see Fig. 14B), and that is accessible to an effective synergistic promotion by cobalt. At higher loadings from about 15 wt.% up to the saturation loading, the molybdena species are mostly adsorbed by physical interactions in micropores in a 'multilayer' form that does not influence the surface properties and that is not accessible to an effective synergistic promotion by cobalt.

Furthermore, cobalt hydroxide carbonate as the impregnation compound by SAS gained successful and high promotional effect in HDS activity 16-21. Furthermore, the HDS activity of activated carbon-supported Mo and CoMo sulfide catalysts is much higher than that of their alumina-supported counterparts. The high surface area S_{BET} or S_M (as an extensive factor) of activated carbons is not the main reason for this high activity because the surface area of carbon-supported catalysts evaluated by a modified BET method (recommended in the literature for microporous solids) is not much higher than the surface area of alumina-supported catalysts.

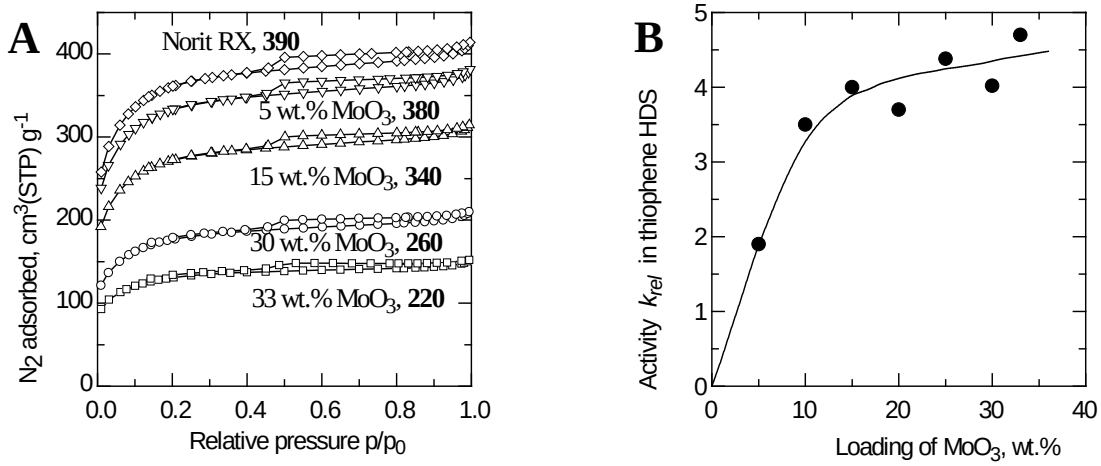

Fig. 14: Adsorption isotherms for N_2 adsorption (**A**) and the dependence of the relative hydrodesulfurization activity k_{rel} on the actual loading over the MoO_3/C(Norit RX) catalyst (**B**). The reference catalyst was the MoO_3/Al_2O_3 catalyst BASF M8-30. Numbers in (A) means V_{micro} in mm^3g^{-1}. [O1]

7. HDS catalysts supported on magnesia

Unlike all the other discussed supports, high surface area MgO (150-300 m^2g^{-1}) is chemically and texturally unstable under aqueous impregnation conditions. It is deeply hydrated to low surface area $Mg(OH)_2$ and partially dissolved at the natural pH of the aqueous $(NH_4)_6Mo_7O_{24}$ solution. Nevertheless, within our group, we have reported that high surface area MoO_3/MgO catalysts can be prepared by the reaction of high surface area MgO (S_{BET} 250–300 $m^2\ g^{-1}$) with a slurry of MoO_3 in methanol [171]. This modification of SAS was named methanol-assisted spreading [O8]. In the field of HDS, higher basicity of MgO support in comparison to conventionally used γ-Al_2O_3 results in higher dispersion and activity of deposited MoS_2[172], higher synergy in CoMo phase [O3] and higher endurance to coking [173]. Apart from a low hydrothermal stability of MgO, its mechanical properties may also restrict the support to be used in industrial HDS fixed-bed applications [29].

Nonetheless, the motivation to achieve high HDS activities led our effort to elucidate on possibility of deposition of molybdenyl- and cobalt- acetylacetonates on the high surface area MgO by impregnation from solutions of these compounds in methanol. Furthermore, dimethylsulfoxide solutions of MoO_3 and $CoCO_3$, $(NH_4)_6Mo_7O_{24}$ and $Co(NO_3)_2$, or $MoO_2(C_5H_7O_2)_2$ and $Co(C_5H_7O_2)_2$ with chelating agent nitrilotriacetic acid (NTA) were studied for CoMo deposition in one impregnation step. This approach represents an analogy to previously introduced chelating agent assisted spreading. Selected impregnation methods were studied also over a new commercially available high surface area nano-MgO support with S_{BET} = 504 m^2g^{-1}, S_M = 420 m^2g^{-1}, and V_{micro} = 53 mm^3g^{-1}. [O22]

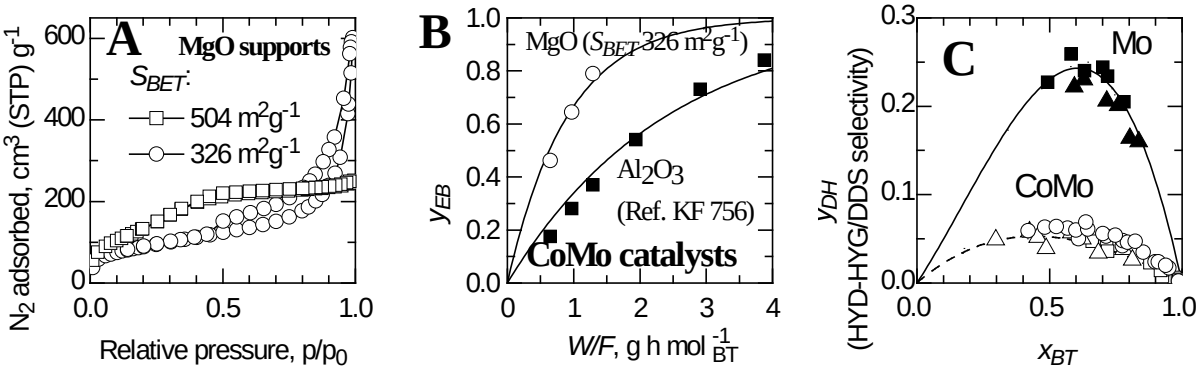

Fig. 15: Nitrogen adsorption-desorption isotherms of the supports (**A**); an example of the activity of MgO supported catalyst (open circles) prepared by deposition of Co acetylacetonate onto sulfided Mo species and commercial Al_2O_3 supported catalysts (**B**); and selectivity to dihydrobenzothiophene (DH) during 1-benzothiophene (BT) HDS (**C**): solid line – Mo/Al_2O_3 (BASF); dash line – CoMo/Al_2O_3 (KF756); solid squares – Mo catalysts over MgO of S_{BET} 326 m^2g^{-1}; solid triangles – Mo catalysts over MgO of S_{BET} 504 m^2g^{-1}; open circles – CoMo catalysts (prepared without NTA) over MgO of S_{BET} 326 m^2g^{-1}; open squares – CoMo catalysts prepared with NTA over MgO of S_{BET} 326 m^2g^{-1}; open triangles – CoMo catalysts (prepared without NTA) over MgO of S_{BET} 504 m^2g^{-1}. [O22]

It has been shown that the nano-MgO with surface area S_{BET} = 504 m^2g^{-1} was able to disperse higher loading of Mo in comparison with home-made MgO of S_{BET} = 326 m^2g^{-1}, S_M = 280 m^2g^{-1}, and V_{micro} = 25 mm^3g^{-1}, which resulted in a correspondingly higher activity in HDS of benzothiophene. Impregnation of the supports with methanolic solution of molybdenyl acetylacetonate reduced mainly the operation time in comparison to previously reported and rather delicate method called methanol-assisted spreading of MoO_3 [O8] while keeping the same HDS activity and HYD-HYG/DDS selectivity, see Fig. 15. Deposition of Co, however, showed on textural instability of the MgO support with the original S_{BET} = 504

m^2g^{-1}. The MgO with S_{BET} = 326 m^2g^{-1} was the support yielding the highest activity of CoMo in HDS. Apart from previously reported deposition of cobalt nitrate from methanolic solution onto MoO_3/MgO catalysts [O3], the most active catalysts were prepared by (i) deposition of cobalt acetylacetonate from methanolic solution onto dried form of MgO supported molybdenyl acetylacetonate followed by calcination, or (ii) deposition cobalt acetylacetonate from methanolic solution onto pre-sulfided Mo/MgO catalysts followed by sulfidation, or (iii) co-impregnation of the MgO with solution made by dissolution of cobalt acetylacetonate, molybdenyl acetylacetonate and chelating agent nitrilotriacetic acid (molar ratio NTA/(Co + Mo) = 1) in dimethylsulfoxide though this third approach is not recommended due to problematic drying. The CoMo/MgO catalysts exhibited at least 3.3-fold activities but the same relative selectivity C=C hydrogenation/C-S hydrogenolysis as the reference industrial CoMo/Al_2O_3 catalyst. [O22]

8. HDS catalysts supported on silica-alumina

The SiO_2-Al_2O_3 support with acidic properties was mostly investigated as a support of novel Pd(Pt) phase [18-21] (see below Section 10) but the SAS method was also successfully applied for CoMo deposition [O19]. This method belongs to the group of methods of MoO_3/SiO_2–Al_2O_3 preparations alternative to conventional impregnation that include modification of the impregnation solution by the addition of chelating agents [174], using hydrogen peroxide to dissolve metallic Mo before impregnation [57], thermal spreading of MoO_3 over SiO_2–Al_2O_3 support at temperatures about 500 °C [175,176], flame spray pyrolysis of molybdenum 2-ethylhexanoate, hexamethyldisiloxane and aluminium acetylacetonate [56], or coprecipitation of $(NH_4)_6Mo_7O_{24}$, Na_2SiO_3 and $Al_2(SO_4)_3$ from aqueous solution at controlled pH [66,67].

It was found that the water-assisted spreading method (SAS) is suitable for the deposition of MoO_3 onto the acidic SiO_2–Al_2O_3 supports. However, the MoO_3 loading L_a depended on the Al_2O_3 content in the SiO_2–Al_2O_3 supports. The precipitated and washed SiO_2–Al_2O_3 and the dealuminated SiO_2–Al_2O_3s (SiO_2–Al_2O_3 modified with nitric acid leaching) contained 52, and 33, and 19 wt.% of Al_2O_3, respectively, and exhibited PZC of 6.3, 4.5, and 4.4, respectively. The surplus of MoO_3 applied during saturation experiments caused further dealumination to result in the actual content of Al_2O_3 and MoO_3 34 and 17.1 wt.%, 19 and 7.2 wt.%, and 12 and 3.1 wt.%, respectively. Considering the relatively high surface area S_{NE} of original support and resultant catalysts, i.e. 429 and 255; 580 and 683; and 600 and 680 m^2g^{-1}, respectively, the L_as were lower than it was observed for all oxidic supports discussed above. The above mentioned linear correlation between actual loadings of MoO_3 and the actual Al_2O_3 content could be presumably explained by the fact that MoO_3 adsorbed onto Al containing site of these supports, which were positively charged and adsorbed the negatively charged dissolved Mo species from the acidic slurry MoO_3/H_2O (pH about 2.5).

The deposited phase, moreover, was found to be X-ray amorphous and only the ´interaction´species of polymolybdates with the support [57,177] were found by Raman spectroscopy in Fig. 16A. The deposited and sulfided Mo species are accessible for the promotion of the HDS activity by Co. It was concluded that the modified SiO_2–Al_2O_3 by acid leaching is a promising support for the sulfidic CoMo phase to achieve high intrinsic HDS activities. The acidic properties of the modified SiO_2–Al_2O_3 supports in terms of cyclohexene isomerization and cumene cracking are preserved after deposition of the sulfidic CoMo phase as is shown in Fig. 16B. The main factor influencing these properties was found to be the Al_2O_3 content. The precise elucidation on the optimal Al_2O_3 content in modified SiO_2–Al_2O_3 to achieve high HDS activity and to keep high acidity should be subject of further research.[O19]

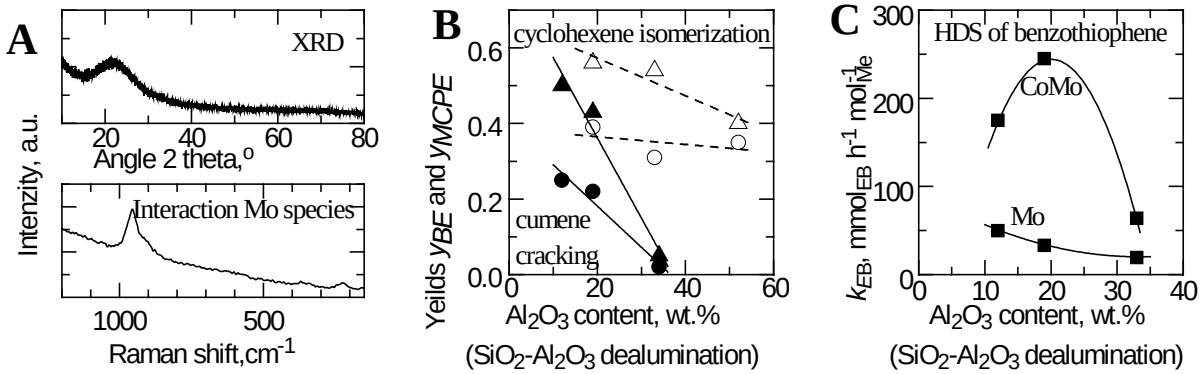

Fig. 16: X-ray diffraction (XRD) patterns and Raman spectra of CoMo catalysts with 17 wt.% of Al_2O_3 in SiO_2–Al_2O_3 support after impregnation and drying at 95 °C; (**A**); dependence of cumene cracking and cyclohexene isomerization (**B**) the HDS activity k_{EB} (**C**) on Al_2O_3 content in the supports: supports (open points, dash lines) and sulfide CoMo catalysts (filled points, solid lines); yields of benzene y_{BE} (filled circles) and methylcyclopentene y_{MCP}E (filled triangles); and intrinsic (normalized per mol of Mo or Co+Mo) HDS activity k_{EB} (filled squares). [O19]

9. Comparison of shaped catalysts

The overview of alternative supports of HDS catalysts [178] and other innovation of hydroprocessing could be found elsewhere [31]. Nevertheless, most of the scientific papers in the field deal with catalysts and supports in the form of grains despite the fact that industrial scale processes require shaped forms such as extrudates or tablets. SAS of shaped forms of selected supports (formation of eggshell Mo profiles before reaching homogeneous profiles) was addressed above in Section 5.1. The comparison of how microstructural properties of extrudates such as S_{BET}, S_M, V_{micro}, ρ_{He} (skeletal density), ρ_{Hg} (envelope density), ε (porosity), and $\langle r \rangle$ (mean transport pore radius [179-181]) depends on the deposition of MoO_3 and $CoCO_3.Co(OH)_2$ (dried form of catalysts) and sulfidation (sulfidic $CoMoS_2$ form of catalysts) are summarized here [O25]. About 300 pieces of the extrudates of activated carbon (Norit RX), Al_2O_3, TiO_2 and ZrO_2 of the same external diameter corresponding to 3.2 mm were cut to the uniform length of 5 mm and utilized for this study. The HDS of benzothiophene, however, was measured of the catalysts in the form of grain 0.16-0.33 mm. The weight normalized values of k_{EB} 122, 142, 383, and 749 $mmol_{EB}$ g^{-1} h^{-1} for the ZrO_2, TiO_2, Al_2O_3,and C supported CoMo catalysts corresponded to promotional effect k_{EB}(CoMo)/ k_{EB}(Mo) 4.1, 3.6, 7.3, and 8.3, respectively. After normalization to bed volume using experimentally determined packing densities 1.24, 0.9, 0.7, and 0.62, the k_{EB}s were 151, 128, 268, and 464 $mmol_{EB}$ cm^{-3} h^{-1}, respectively. Fig 17A correlates activities in HDS to mean transport pore radii of supports $\langle r \rangle$, S_{BET}s of supports and the achieved saturated adsorption loadings $L_a^{CoO+MoO3}$. Fig. 17B qualitatively compares SAS of MoO_3 over shaped supports and it includes also Al_2O_3 spherical pellets or extrudates of different diameters.

It was concluded that the support effect, represented in the present work by S_{BET}, L_a and mainly by the mean transport-pore radius $\langle r \rangle$, govern resultant activity of CoMo catalysts. The increasing mean transport-pore radii either of the support or of the sulfide catalyst correlated well qualitatively with the increasing activity in HDS of 1-benzothiophene in the order: $ZrO_2 \sim TiO_2 < Al_2O_3 <$ C (Fig. 20A). Nevertheless, according to both microstructural analysis and HDS activity study, the supports and catalysts could be selected into two main groups. The first group, ZrO_2- and TiO_2-based systems, exhibited low microstructural changes in terms of textural and transport characteristics after deposition of CoMo (both in oxidic and sulfide stage) onto the supports, relatively narrow mean transport-pore radii between 19-33 nm, and low HDS activities of CoMo catalysts (both weight and

volume normalized activities). In contrast, the second group, Al_2O_3- and C-based systems, revealed significant changes in microstructure after deposition of the CoMo phases onto the supports, but exhibited wider mean transport-pore radii ranging from 40 to 221 nm, and more than 1.8 times higher HDS activities of CoMo catalysts than the first group. The activated carbon supported CoMo catalyst exhibited the highest HDS activity and the mean transport-pore radius despite the highest volume of micropores, which emphasized relevancy of further research. [O25]

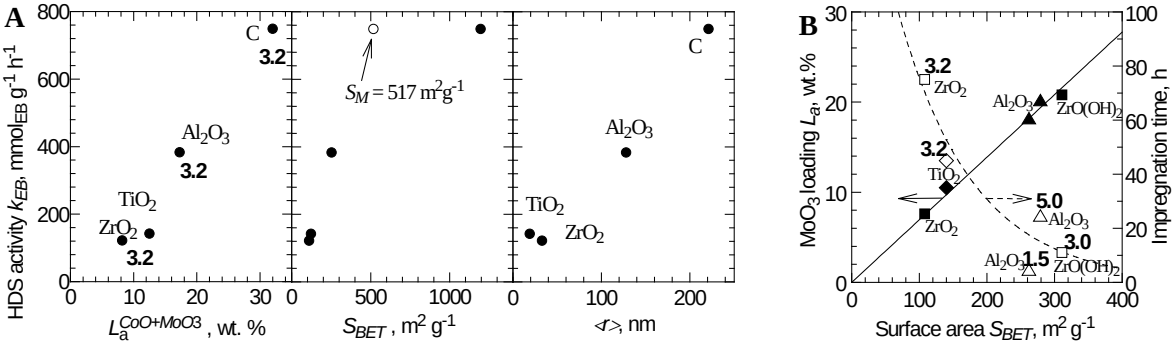

Fig. 17: Empiric correlation of the CoMo loadings $L_a^{CoO+MoO3}$, support surface area S_{BET} and support mean transport-pore radius <*r*> with the HDS activity k_{EB} (**A**) [O25] and the dependence of saturated adsorption loadings of MoO_3 L_a (solid line and filled symbols) and impregnation time needed for the saturation by SAS at 95 °C (dashed line and open symbols) on the surface areas S_{BET} of the supports (**B**) [O16]: squares – ZrO_2 and $ZrO(OH)_2$, diamonds – TiO_2 [O7], and triangles – Al_2O_3 [O2], the numbers - the external diameters in mm of the extrudates or balls studied.

10. Novel active phases

Novel active phases attract attention of fundamental research to increase hydrotreating activity or to modify reactivity of conventionally used Co(Ni)Mo counterparts. For these reasons, novel phases are studied in our works i) as individual metal or sulfide supported on varieties of carriers [O15, O39, 18, 22, 23] or ii) in their mixed phases [19-21] or iii) as an activity promoter of conventional Mo species [O3, 24-27]. Within noble metals, the price often predetermines low loadings of metals and consequently their use as activity promoters [24,27]. In this section, only those results achieved with realtion to SAS method are briefly outlined.

The research on ability of carbon based supports to adsorb high amounts of transition metals (for Mo see Section 6) was explored also for the synthesis of highly loaded Pt/C electrocatalysts. The catalysts consisting of 60 wt.% of Pt were prepared by one-step impregnation of the studied high-surface-area carbon black ENSACO® 350G of S_{BET} = 808 m^{2}g^{-1}, S_M = 419 m^{2}g^{-1}, V_{micro} = 196 mm^{3}g^{-1}, and *d(G,Raman)* = 5 nm using PtO_2 (SAS, i.e. PtO_2/H_2O slurry) , H_2PtCl_6 (solution impregnation), $Pt(C_5H_7O_2)_2$ (SAS, i.e. slurries with organic solvents), $Pt(NH_3)_4(NO_3)_2$(solution impregnation), and $Pt(NH_3)_2(NO_2)_2$ (solution impregnation). The species were reduced to metallic Pt at 0, 70, 120, 140, and 150 °C, respectively, as it was followed by TPR. Calcination in Ar followed by the reduction in an H_2/Ar mixture at 190 °C ranked these catalysts in the following order of increasing Pt particle size *d(Pt,H$_2$)*: 3 < 8 < 11-17 ~ 16 < 18-35 nm for the precursor H_2PtCl_6, $Pt(NH_3)_2(NO_2)_2$, $Pt(C_5H_7O_2)_2$, $Pt(NH_3)_4(NO_3)_2$, PtO_2, respectively, favoring H_2PtCl_6. The selected catalysts were characterized comprehensively. [O23, 5-7]

It was concluded that SAS could be explored to deposition of PtO_2 to synthesize carbon blacks supported eletrocatalysts [O23]. Though the dispersion was poor presumably due to overloading of the supports, the SAS could be successful at lower loadings, below 30-40 wt.%, for the electrocatalysts for fuel cell or CO_2 reduction applications or at loadings below 1 wt.% if the Pt would be used as an activity promoter in other reactions such as hydrorefining.

11. Conclusions

It has been shown that the Solvent-Assisted Spreading (SAS) method is suitable for the deposition of MoO_3 onto Al_2O_3, ZrO_2, TiO_2, MgO, SiO_2-Al_2O_3, and C supports. Co and Ni can be deposited over catalysts containing saturated adsorption monolayer of MoO_3 by SAS, i.e. from aqueous slurries of low solubility carbonates or hydroxycarbonates. The SAS method does not make it possible to exceed the dispersion capacity of the support surface. This method is a clean and simple method of Co(Ni)Mo deposition, which does not introduce any auxiliary ions like NH_4^+ or NO_3^-; furthermore, calcination is not needed. Excluding of the calcination step is particularly important during preparation of C supported catalysts due to the propensity of C to burn. Methanol instead of water is used as a solvent during impregnation of hydrothermally unstable supports MgO and mesoporous organized Al_2O_3. Only water or methanol is produced during drying. Water or methanol represent the only side products of SAS. The SAS method thus belongs to the group of green chemistry and conforms to sustainable development.

It has been shown on the shaped forms of supports that an eggshell radial profile of Mo concentration is formed by SAS. The thickness of the eggshell can be efficiently regulated by the amount of MoO_3 used. Moreover, CoMo and NiMo active phases can be added to α-boehmite paste, using the principles of SAS, before shaping. The sequential reaction of α-boehmite with MoO_3 and then Co or Ni carbonates in an aqueous paste leads to increased textural stability of Al_2O_3 during calcination. The catalysts prepared by SAS are at least as active and selective in model HDS reactions as the reference commercial or conventionally prepared counterparts.

It has been shown that the modification of SAS using the chelating agent nitrilotriacetic acid, NTA, allows effective deposition of Co(Ni)Mo avoiding addition of NH_4OH, which is normally used. Novel active phases for hydrorefining reactions or oxygen reduction reactions for fuel cell application have been investigated. Many factors must be monitor carefully in order to prepare heterogeneous catalysts active and selective in a particular reaction. These factors are specific chemistry of each individual supports and catalysts such as content of Na, Ca, or Cl admixture (the sample history), as well as structural, textural and transport parameters such as crystalic structure, surface area, microporosity, or mean transport pore radii.

SAS method utilized the surface area of Al_2O_3, OMA, ZrO_2, $ZrO(OH)_2$, TiO_2, MgO and nano-MgO support, i.e. the extensive factor, yielding saturated adsorption monolayer of approximately 3.5 Mo nm^{-2}. The other two support of high surface area (C and SiO_2-Al_2O_3) differed. Activated carbons (C) adsorbed high amounts of Mo but only about half of it has properties of monolayer while the rest was deposited as a multilayer in micropores. Silica-aluminas yielded rather tentative values of surface Mo densities 0.2-2.0 Mo nm^{-2}. Nevertheless, the saturated adsorption loading of Mo well correlated with the Al_2O_3 content in SiO_2-Al_2O_3, i.e. the factor of quality.

The main effect that influences the resultant HDS activity of the studied catalysts is summarized in Table 6. The activity of all Al_2O_3-based catalysts studied is deeply influenced by the extensive factor of surface area. The higher surface area leads to higher Mo or Co(Ni)Mo loadings and higher HDS activities. The extensive factor is also clearly

pronounced for Mo catalysts deposited onto all MgO supports studied. The intrinsic activity of Mo is the same over MgO as over Al_2O_3.

In contrast, the factor of quality (composition) is leading in the case of all the other support types. More specifically, the structural properties of ZrO_2 and TiO_2, i.e. the factor of quality, influenced HDS activities. Only monoclinic form of ZrO_2 (baddeleyite) and tetragonal form of TiO_2 (anatase) led to highly active catalysts. The intrinsic activity of Mo was more than two fold in comparison to Al_2O_3. Amorphous hydrous zirconia $ZrO(OH)_2$ and nano-TiO_2 appeared inconvenient despite high surface area and high loadings.

Furthermore, the qualitative factor is highly pronounced over all carbon supported catalysts. Activity of Mo and CoMo catalysts overhelmed the Al_2O_3 supported counterparts more than 3 fold. Similar phenomenon was observed for MgO-supported CoMo catalysts. The high surface area of the supports determined by standard BET method , S_{BET}, can hardly explain that behavior. If the surface area is evaluated by modified BET method, S_M (the method recommended in the literature to achieve physically more realistic values), the factor of quality is even more pronounced.

Table 6: Determinant factors of high HDS activity of the prepared catalysts

	Extensive factor (S_{BET})		Factor of quality (composition)	
	Mo	Co(Ni)Mo	Mo	Co(Ni)Mo
Al_2O_3	+	+		
OMA	+	+		
αAlOOH	+	+		
ZrO_2			+	+
TiO_2			+	+
nanoTiO_2			+	
C			+	+
MgO	+			+
nanoMgO	+			+
SiO_2-Al_2O_3			+	+

Original papers used in this thesis

O1. Kaluža L., Zdražil M.: Carbon-Supported Mo Catalysts Prepared by a New Impregnation Method Using a MoO3/Water Slurry: Saturated Loading, Hydrodesulfurization Activity and Promotion by Co. Carbon 39(13), 2023-2034 (2001).

O2. Kaluža L., Zdražil M.: Preparation of MoO3/Al2O3 Catalysts with Sharp Eggshell Mo Distribution by Slurry Impregnation. Catal. Lett. 78(1-4), 313-318 (2002).

O3. Vít Z., Gulková D., Kaluža L., Zdražil M.: Effect of Support on the Synergy in HDS of Thiophene and HDN of Pyridine over Mo Sulfide Catalysts Promoted by Rh. React. Kinet. Catal. Lett. 83(2), 237-244 (2004).

O4. Kaluža L., Vít Z., Zdražil M.: Preparation and Properties of Filled Monolayer of MoO3 Deposited on Al2O3 Supports by Solvent-Assisted Spreading. Appl. Catal., A 282(1-2), 247-253 (2005).

O5. Kaluža L., Zdražil M.: Preparation of MoO3/gamma-Al2O3 Catalyst by the Reaction of alpha-Boehmite with MoO3/H2O Slurry - Dual Role of MoO3 as Active Phase and Texture Stabilizer during Calcination. React. Kinet. Catal. Lett. 85(2), 391-398 (2005).

O6. Zdražil M., Kaluža L., Gulková D.: Preparation of Eggshell MoO3/Al2O3 Catalysts by Solvent Assisted Spreading of MoO3 over Al2O3 Extrudates: Effect of MoO3

Particle Size and Temperature on Rate of Spreading. Mat. Sci.: An Indian J. 1(1-2), 1-10 (2005).
O7. Gulková D., Kaluža L., Vít Z., Zdražil M.: Preparation of MoO3/TiO2 Catalysts with Eggshell and Uniform Mo Distribution by Water-Assisted Spreading of MoO3. Catal. Lett. 112(3-4), 193-196 (2006).
O8. Gulková D., Kaluža L., Vít Z., Zdražil M.: Preparation of MoO3/MgO Catalysts with Eggshell and Uniform Mo Distribution by Methanol Assisted Spreading: Effect of MoO3 Dispersion on Rate of Spreading. Catal. Commun. 7(5), 276-280 (2006).
O9. Kaluža L., Gulková D., Vít Z., Zdražil M.: Effect of Support Type on the Magnitude of Synergism and Promotion in CoMo Sulphide Hydrodesulphurisation Catalyst. Appl. Catal., A 324, 30-35 (2007).
O10. Kaluža L., Zdražil M.: Deposition of CoO onto MoO3/Al2O3 Hydrodesulfurization Catalysts by Solvent Assisted Spreading. Top. Catal. 45(1-4), 191-194 (2007).
O11. Kaluža L., Zdražil M.: Preparation of Bimetallic CoO-MoO3/gamma-Al2O3 and NiO-MoO3/ gamma-Al2O3 Hydrodesulfurization Catalysts by Deposition of Co, Ni, and Mo onto alpha-AlOOH during Paste Processing. Reac. Kinet. Catal. Lett. 91(2), 249-255 (2007).
O12. Kaluža L., Zdražil M.: Preparation of Zirconia-Supported Hydrodesulphurisation Catalysts by Water-Assisted Spreading. Appl. Catal., A 329, 58-67 (2007).
O13. Gulková D., Kaluža L., Vít Z., Horáček J., Macháčková E., Zdražil M.: High Surface Area MoO3/TiO2 Hydrodesulfurization Catalysts. Reac. Kinet. Catal. Lett. 94(2), 219-226 (2008).
O14. Kaluža L., Gulková D., Šolcová O., Žilková N., Čejka J.: Hydrotreating Catalysts Supported on Organized Mesoporous Alumina: Optimization of Mo Deposition and Promotional Effects of Co and Ni. Appl. Catal., A 351(1), 93-101 (2008).
O15. Kaluža L., Zdražil M.: The Effect of gamma-Al2O3, TiO2, and ZrO2 Supports on Hydrodesulfurization Activity of Transition-Metal Sulfides. Collect. Czech. Chem. Commun. 73(8-9), 945-955 (2008).
O16. Kaluža L., Zdražil M.: Slurry Impregnation of ZrO2 Extrudates: Controlled EggShell Distribution of MoO3, Hydrodesulfurization Activity, Promotion by Co. Catal. Lett. 127(3-4), 368-376 (2009).
O17. Kaluža L., Zdražil M., Vít Z.: Deposition of NiO onto MoO3/gamma-Al2O3 Extrudates by Slurry Impregnation Method. Reac. Kinet. Catal. Lett. 97(2), 307-313 (2009).
O18. Kaluža L., Gulková D., Vít Z., Zdražil M.: CoMo/ZrO2 Hydrodesulfurization Catalysts Prepared by Chelating Agent Assisted Spreading. Catal. Lett. 142(8), 969-974 (2012).
O19. Kaluža L., Gulková D., Vít Z., Zdražil M.: Water-Assisted Spreading of MoO3 onto SiO2-Al2O3 Supports for Preparation of Sulfide CoMo Hydrodesulfurization Catalysts. Fuel 112, 272-276 (2013).
O20. Kaluža L., Zdražil M., Gulková D., Vít Z.: The Influence of the Chelating Agent Nitrilotriacetic Acid on Promotion of Hydrodesulfurization Activity by Co in CoMo Catalysts Prepared on Al2O3, C, and ZrO2 Supports. Chem. Eng. Trans. 32(2), 841-846 (2013).
O21. Kaluža L.: Activity of Transition Metal Sulfides Supported on Al2O3, TiO2 and ZrO2 in the Parallel Hydrodesulfurization of 1-Benzothiophene and Hydrogenation of 1-Methyl-Cyclohex-1-Ene. Reac. Kinet. Mech. Cat. 114(2), 781-794 (2015).
O22. Kaluža L., Gulková D., Vít Z., Zdražil M.: High-activity MgO-supported CoMo Hydrodesulfurization Catalysts Prepared by Non-aqueous Impregnation. Appl. Catal. B-Environ. 162, 430-436 (2015).

O23. Kaluža L., Larsen M.J., Zdražil M., Gulková D., Vít Z., Šolcová O., Soukup K., Koštejn M., Bonde J.L., Maixnerová L., Odgaard M.: Highly Loaded Carbon Black Supported Pt Catalysts for Fuel Cells. Catal. Today 256, 375-383 (2015).

O24. Kaluža L., Zdražil M.: Relative activity of Niobia-supported CoMo hydrodesulphurization catalyst prepared with NTA: A kinetic approach. Catal. Commun. 107, 62–67 (2018).

O25. Soukup K., Procházka M., Kaluža L.: Microstructural Properties and HDS Activity of CoMo Catalysts Supported on Activated Carbon, Al2O3, ZrO2 and TiO2. 12 International Conference on Chemical and Process Engineering - ICheaP12, Chem. Eng. Trans., Volume 43, pp. 841-846, 2015, Milano, Italy, 19-22 May 2015.

References: (no. –the author as a coauthor, [no] - other)

1. Kaluža L., Zdražil M., Žilková N., Čejka J.: High Activity of Highly Loaded MoS2 Hydrodesulfurization Catalysts Supported on Organised Mesoporous Alumina. Catal. Commun. 3, 151-157 (2002).
2. Čejka J., Žilková N., Kaluža L., Zdražil M.: Mesoporous Alumina as a Support for Hydrodesulfurization Catalysts. 3rd International Symposium on Nanoporous Materials, Stud. Surf. Sci. Catal., Volume 141, pp. 243-250, Ottawa, Ontario, Canada, 12-15 June 2002.
3. Kubička D., Kaluža L.: Deoxygenation of Vegetable Oils over Sulfided Ni, Mo and NiMo Catalysts. Appl. Catal., A 372(2), 199-208 (2010).
4. Kaluža L., Kubička D.: The comparison of Co, Ni, Mo, CoMo and NiMo sulfided catalysts in rapeseed oil hydrodeoxygenation. React. Kinet. Mech. Cat. 122(1), 333–341 (2017).
5. Kaluža L., Larsen M.J., Zdražil M., Gulková D., Odgaard M.: Fuel Cell Platinum Catalysts Supported on Mediate Surface Area Carbon Black Supports. 12 International Conference on Chemical and Process Engineering - ICheaP12, Chem. Eng. Trans., Volume 43, pp. 913-918, 2015, Milano, Italy, 19-22 May 2015.
6. Kaluža L., Larsen M.J., Morales I.J., Cavaliere S., Jones D.J., Roziere J., Kallistová A., Dytrych P., Gulková D., Odgaard M.: Synthesis of Pt/C Fuel Cell Electrocatalysts: Residual Content of Chloride and Activity in Oxygen Reduction. Electrocatalysis 7(4), 269-275 (2016).
7. Larsen M.J., Morales I.J., Cavaliere S., Zajac J., Jones D.J., Rozière J., Kaluža L., Gulková D., Odgaard M.: Development of Tailored High-Performance and Durable Electrocatalysts for Advanced PEM Fuel Cells. Int. J. Hydrog. Energy 42(10), 7166-7176 (2017).
8. Palcheva R., Kaluža L., Dimitrov L., Tyuliev G., Avdeev G., Jirátová K., Spojakina A.: NiMo Catalysts Supported on the Nb Modified Mesoporous SBA-15 and HMS: Effect of Thioglycolic Acid Addition on HDS. Appl. Catal., A 520, 24-34 (2016).
9. Spojakina A.A., Jirátová K., Novák V., Palcheva R., Kaluža L.: Hydrodesulfurization of Different Feeds on CoMo/Al2O3 Catalyst Prepared Using Cobalt Heteropolyoxomolybdate. Collect. Czech. Chem. Commun. 73(8-9), 983-999 (2008).
10. Palcheva R., Spojakina A.A., Jirátová K., Kaluža L.: Effect of Co on HDS Activity of Alumina-supported Heteropolymolybdate. Catal. Lett. 137(3-4), 8 (2010).
11. Palcheva R., Kaluža L., Spojakina A., Jirátová K., Tyuliev G.: NiMo/γ-Al2O3 Catalysts from Ni Heteropolyoxomolybdate and Effect of Alumina Modification by B, Co, or Ni. Chin. J. Catal. 33(4-6), 952-961 (2012).
12. Jirátová K., Spojakina A., Kaluža L., Palcheva R., Balabánová J., Tyuliev G.: Hydrodesulfurization Activities of NiMo Catalysts Supported on Mechanochemically Prepared Al-Ce Mixed Oxides. Chin. J. Catal. 37(2), 258–267 (2016).
13. Žáček P., Kaluža L., Karban J., Storch J., Sýkora J.: The Rearrangement of 1-Methylcyclohex-1-ene during the Hydrodesulfurization of FCC Gasoline over Supported Co(Ni)Mo/Al2O3 Sulfide Catalysts: the Isolation and Identification of Branched Cyclic C7 Olefins. React. Kinet. Mech. Cat. 112(2), 335-346 (2014).
14. Gaálová J., Topka P., Kaluža L., Šolcová O.: Gold versus Platinum on Ceria-Zirconia Mixed Oxides in Oxidation of Ethanol and Toluene. Catal. Today 175(1), 231-237 (2011).

15. Matějová L., Topka P., Kaluža L., Pitkäaho S., Ojala S., Gaálová J., Keiski R.L.: Total Oxidation of Dichloromethane and Ethanol over Ceria-Zirconia Mixed Oxide Supported Platinum and Gold Catalysts. Appl. Catal. B-Environ. 142– 143, 54– 64 (2013).
16. Topka P., Delaigle R., Kaluža L., Gaigneaux E.M.: Performance of Platinum and Gold Catalysts Supported on Ceria-Zirconia Mixed Oxide in the Oxidation of Chlorobenzene. Catal. Today 253, 172-177 (2015).
17. Topka P., Kaluža L., Gaálová J.: Total Oxidation of Ethanol and Toluene over Ceria-Zirconia Supported Platinum Catalysts. Chem. Pap. 70(7), 898-906 (2016).
18. Vít Z., Gulková D., Kaluža L., Bakardieva S., Boaro M.: Mesoporous Silica-alumina Modified by Acid Leaching as Support of Pt Catalysts in HDS of Model Compounds. Appl. Catal., B 100(3-4), 463-471 (2010).
19. Vít Z., Kmentová H., Kaluža L., Gulková D., Boaro M.: Effect of Preparation of Pd and Pd-Pt Catalysts from Acid Leached Silica-Alumina on Their Activity in HDS of Thiophene and Benzothiophene. Appl. Catal., B 108(1-2), 152-160 (2011).
20. Vít Z., Gulková D., Kaluža L., Boaro M.: Effect of Catalyst Precursor and Its Pretreatment on the Amount of ß-Pd Hydride Phase and HDS Activity of Pd-Pt/Silica-Alumina. Appl. Catal. B-Environ. 146, 213– 220 (2014).
21. Vít Z., Gulková D., Kaluža L., Kupčík J.: Pd-Pt Catalysts on Mesoporous SiO2-Al2O3 with Superior Activity for HDS of 4,6-Dimethyldibenzothiophene: Effect of Metal Loading and Support Composition. Appl. Catal. B-Environ. 179, 44-53 (2015).
22. Gulková D., Kaluža L., Vít Z., Zdražil M.: Support Effect in Hydrodesulfurization over Ruthenium Sulfide. Petroleum and Coal 51(2), 146-149 (2009).
23. Kaluža L., Vít Z., Zdražil M.: Support Effect in the Hydrodesulfurization of Thiophene over Rhodium Sulfide. React. Kinet. Mech. Cat. 101(1), 63-72 (2010).
24. Vít Z., Gulková D., Kaluža L., Zdražil M.: Synergetic Effects of Pt and Ru Added to Mo/Al2O3 Sulfide Catalyst in Simultaneous Hydrodesulfurization of Thiophene and Hydrogenation of Cyclohexene. J. Catal. 232(2), 447-455 (2005).
25. Vít Z., Kaluža L., Gulková D.: Nitrogen Tolerant Hydrodesulfurization Catalysts Based on Rh and Ru Promoted Mo/Al2O3. Top. Catal. 54(16-18), 1325-1330 (2011).
26. Vít Z., Kaluža L., Gulková D.: Comparison of Nitrogen Tolerance of PdMo/Al2O3 and CoMo/Al2O3 Catalysts in Hydrodesulfurization of Model Compounds. Fuel 120, 86-90 (2014).
27. Kaluža L., Gulková D.: Effect of Promotion Metals on the Activity of MoS2/ZrO2 Catalyst in the Parallel Hydrodesulfurization of 1-Benzothiophene and Hydrogenation of 1-Methyl-Cyclohex-1-ene. React. Kinet. Mech. Catal. 118(1), 313–324 (2016).
28. Kaluža L., Zdražil M.: Niobia Supported Mo Sulfide Hydrodesulfurization Catalysts Prepared Using Nitrilotriacetic Acid. Current Topics in Catalysis 11, 65-74 (2014).
[29] Toulhoat H., Raybaud P., Catalysis by Transition Metal Sulphides, Editions Technip, Paris, France (2013).
[30] Eijsbouts S., Mayo S.W., Fujita K., Appl. Catal. A 322, 58-66 (2007).
[31] Leliveld R.G., Eijsbouts S., Catal. Today 130, 183-189 (2008).
[32] Brown A.C.S., Hargreaves J.S.J., Taylor S.H., Catal. Lett. 57, 109-113 (1999).
[33] Zhang X., He D.H., Zhang Q.J., Ye Q., Xu B.Q., Zhu Q.M., Appl. Catal. A 249, 107-117 (2003).
[34] Brückman K., Grzybowska B., Che M., Tatibouët J.M., Appl. Catal. 96, 279-288 (1993).
[35] Kim D.S., Wachs I.E., Segawa K., J. Catal. 149, 268-277 (1994).
[36] Jin G., Lu G., Guo Y., Guo Y., Wang J., Liu X., Catal. Today, 93–95, 173-182 (2004).
[37] Debecker D.P., Hauwaert D., Stoyanova M., Barkschat A., Rodemerck U., Gaigneaux E.M., Appl Catal A 391, 78-85 (2011).
[38] Vanhove D., Op S.R., Fernandez A., Blanchard M., J. Catal. 57, 253-263 (1979).
[39] Chary K.V.R., Reddy K.R., Kumar Ch.P. Catal. Commun. 2, 277-284 (2001).
[40] Chary K.V.R., Reddy K.R., Kishan G., Niemantsverdriet J.W., Mestl G., J. Catal. 226, 283-291 (2004).
[41] Bhaskar T., Reddy K.R., Kumar C.P., Murthy M.R.V.S., Chary K.V.R., Appl. Catal. 211, 189-201 (2001).

[42] Laniecki M., Malecka-Grycz M., Domka F., Appl. Catal. A 196, 293-303 (2000).
[43] Kanai H., Ikeda Y., Imamura S., Appl. Catal. A 247, 185-191 (2003).
[44] Shimura K., Kanai H., Utani K., Matsuyama K., Inamura S., Appl. Catal. A 283, 117-124 (2005).
[45] Fountzoula Ch., Spanos N., Matralis H.K., Kordulis Ch., Appl. Catal. B 35, 295-304 (2002).
[46] Nova I., Lietti L., Casagrande L., Dall'Acqua L., Giamello E., Forzatti P., Appl. Catal. B 17, 245-258 (1998).
[47] Bourikas K., Fountzoula Ch., Kordulis Ch., Appl. Catal. B 52, 145-153 (2004).
[48] Matralis H., Theret S., Bartians P., Ruwet M., Grange P., Appl. Catal. B 5, 271-281 (1995).
[49] Vrieland G.E., Murchison C.B., Appl. Catal. A 134, 101-121 (1996).
[50] Ogonowski J., Przemysl Chemiczny 65, 657-659 (1986).
[51] Pacheco M.L., Soler J., Dejoz A., López Nieto J.M., Herguido J., Menéndez M., Santamaría J., Catal. Today 61, 101-107 (2000).
[52] Meunier F.C., Yasmeen A., Ross J.R.H., Catal. Today 37, 33-42 (1997).
[53] Chen K., Xie S., Iglesia E., Bell A.T., J. Catal. 189, 421-430 (2000).
[54] Hasegawa S., Tanaka T., Kudo M., Mamada H., Hattori H., Yoshida S., Catal. Lett. 12, 255-266 (1992).
[55] Indovina V., Cimino A., Cordischi D., Della Bella S., De Rossi S., Ferraris G., Gazzoli D., Occhiuzzi M., Valigi M., Stud. Surf. Sci. Catal. 75, 875-887 (1993).
[56] Debecker D.P., Schimmoeller B., Stoyanova M., Poleunis C., Bertrand P., Rodemerck U., Gaigneaux E.M., J. Catal. 277, 154-163 (2011).
[57] Debecker D.P., Stoyanova M., Rodemerck U., Gaigneaux E.M., J. Mol. Catal. A 340, 65-76 (2011).
[58] Debecker D.P., Stoyanova M., Rodemerck U., Leonard A., Su B., Gaigneaux E.M., Catal Today 169, 60-68 (2011).
[59] Lee E.K., Jung K.D., Joo O.S., Shul Y.G., Appl. Catal. A 268, 83-88 (2004).
[60] Reyes P., Fernández J., Concha I., Pecchi G., Catal. Lett. 34, 331-341 (1995).
[61] Yori J.C., Pieck C.L., Parera J.M., Catal. Lett. 64, 141-146 (2000).
[62] Ghosh A.K., Tanaka K., Toyoshima I., J. Catal. 108, 143-152 (1987).
[63] Ghosh A.K., Tanaka K., Toyoshima I., J. Catal. 106, 354-361 (1987).
[64] Aritani H., Shinohara S., Koyama S., Otsuki K., Kubo T., Nakahira A., Chem. Lett. 35, 416-417 (2006).
[65] Hino M., Arata K., Chem. Lett. 18, 971-972 (1989).
[66] Sabu K.R.P., Rao K.V.C., Nair C.G.R., Bull. Chem. Soc. Jpn. 64, 1926-1932 (1991).
[67] Sabu K.R., Rao K.V.C., Indian. J. Chem. 33B, 1053-1061 (1994).
[68] Sohn J.R., Lee S.G., Shin D.C., Bull. Kor. Chem. Soc. 27, 1623-1632 (2006).
[69] Li L., Yoshinaga Y., Okuhara T., Catal. Lett. 83, 231-234 (2002).
[70] Diaz A.L., Bussell M.E., J. Phys. Chem. 97, 470-477 (1993).
[71] Zingg D.S., Makovsky L.E., Tischer R.E., Brown F.R., Hercules D.H., J. Phys. Chem. 84, 2898-2906 (1980).
[72] Van Veen J.A.R., Hendriks P.A.J.M.,. Romers E.J.G.M, Andréa R.R., J. Phys. Chem. 94, 5275-5282 (1990).
[73] Topsøe H., Clausen B.S., Massoth F.E., Hydrotreating Catalysts, Science and Technology, Springer, Berlin (1996).
[74] Heracleous E., Lee A.F., Vasalos I.A., Lemonidou A.A., Catal. Lett. 88, 47-53 (2003).
[75] Vakros J., Bourikas K., Kordulis C., Lycourghiotis A., J. Phys. Chem. B 107, 1804-1813 (2003).
[76] Lycourghiotis A., Stud. Surf. Sci. Catal. 91, 95-129 (1995).
[77] Hillerová E., Morishige H., Inamura K., Zdražil M., Appl. Catal. A 156, 1-17 (1997).
[78] Speight J.G., Lange´s Handbook of Chemistry, McGraw-Hill, New York (2005).
[79] Das K.K., Electrokinetics of mineral particles, in: A.V. Delgado (Ed.), Interfacial Electrokinetics and Electrophoresis, Marcel Dekker, Inc., New York, pp. 799-824 (2002).
[80] Thomazeau C., Martin V., Afanasiev P., Appl. Catal. A 199, 61-72 (2000).
[81] Liu B., Chai Y., Wang Y., Zhang T., Liu Y., Liu C., Appl. Catal. A 388, 248-255 (2010).
[82] Afanasiev P., Appl. Catal A-Gen. 303, 110-115 (2006).

[83] Baston E.P., Franca A.B., Neto A.V.D., Urquieta-Gonzalez E.A., Catal. Today 246, 184-190 (2015).
[84] Baston E.P., Urquieta-Gonzalez E.A., Stud. Surf. Sci. Catal. 175, 671-674 (2010).
[85] Escobar J., Barrera M.C., De Los Reyes J.A., Toledo J.A., Santes V., Colin J.A., J. Mol. Catal. A 287, 33-40 (2008).
[86] Al-Dalama K., Stanislaus A., Thermochim. Acta 520, 67-74 (2011).
[87] Medici L., Prins R., J. Catal. 163, 38-49 (1996).
[88] Palcheva R., Spojakina A., Dimitrov L., Jiratova K., Micropor. Mesopor. Materials, 122, 128-134 (2009).
[89] Ayala M., Esneyder P., Quintana P., Gonzalez-Garcia G., Diaz C., RSC Adv. 5, 102652-102662 (2015).
[90] Cattaneo R., Shido T., Prins R., J. Catal. 185, 199-212 (1999).
[91] Cattaneo R., Weber T., Shido T., Prins R., J. Catal. 191, 225-236 (2000).
[92] Ohta Y., Shimizu T., Homma T., Yamada M., Stud. Surf. Sci. Catal. 127, 161-168 (1999).
[93] Coulier L., De Beer V.H.J., Van Veen J.A.R., Niemantsverdriet J.W., J. Catal. 197, 26-33 (2001).
[94] Van Dillen A.J., Terörde R.J.A.M., Lensveld D.J., Geus J.W., De Jong K.P., J. Catal. 216, 257-264 (2003).
[95] Mochizuki T., Hara T., Koizumi N., Yamada M., Appl. Catal. A 317, 97-104 (2007).
[96] Hensen E.J.M., De Beer V.H.J., Van Veen J.A.R., Van Santen R.A., J. Catal. 215, 353-357 (2003).
[97] Tsuji K., Umeki T., Yokoyama Y., Kitada T., Iwanami Y., Nonaka O., Shimada H., Matsubayashi N., Nishijima A., Nomura M., J. Synchrontron Rad .8, 651-653 (2001).
[98] Rana M.S., Ramírez J., Gutiérrez-Alejandre A., Ancheyta J., Cedeño L., Maity S.K., J. Catal. 246, 100-108 (2007).
[99] Al-Dalama K., Aravind B., Stanislaus A., Appl. Catal. A 296, 49-53 (2005).
[100] Okamoto Y., Ishihara S., Kawano M., Satoh M., Kubota T., J. Catal. 217, 12-22 (2003).
[101] Shimizu T., Hiroshima K., Honma T., Mochizuki T., Yamada M., Catal. Today 45, 271-276 (1998).
[102] Hiroshima K., Mochizuki T., Honma T., Shimizu T., Yamada M., Appl. Surf. Sci. 121/122, 433-436 (1997).
[103] Van Veen J.A.R., Colijn H.A., Hendriks P.A.J.M., Van Welsenes A.J., Fuel Proc. Technol. 35, 137-157 (1993).
[104] Kishan G., Coulier L., Van Veen J.A.R., Niemantsverdriet J.W., J. Catal. 200, 194-196 (2001).
[105] Rana M.S., Captaine E.M.R., Leyva C., Ancheyta J., Fuel 86, 1254-1262 (2007).
[106] Escobar J., Barrera M.C., De Los Reyes J.A., Toledo J.A., Santes V., Colín J.A., J. Mol. Catal. A 287, 33-40 (2008).
[107] Lélias M.A., Van Gestel J., Magué F., Van Veen J.A.R., Catal. Today 130, 109-116 (2008).
[108] Lélias M.A.,Kooyman P.J., Mariey L., Oliviero L., Travert A., Van Gestel J., Van Veen J.A.R., Magué F., J. Catal. 267, 14-23 (2009).
[109] Carrier X., Lambert J.F., Che M., J. Am. Chem. Soc. 119, 10137-10146 (1997).
[110] Carrier X., Lambert J.F., Che M., Stud. Surf. Sci. Catal. 121, 311-316 (1999).
[111] Carrier X., Lambert J.F., Kuba S., Knözinger H., Che M., J. Mol. Struct. 656, 231-238 (2003).
[112] Tuinstra F., Koenig J.L., J. Chem. Phys. 53, 1126–1130 (1970).
[113] Schneider P., Appl. Catal. A 129, 157-165 (1995).
[114] Nelsen F.M., Eggertsen F.T., Anal. Chem. 30, 1387-1390 (1958).
[115] Subramanian S., Schwarz J.A., Hejase Z., J. Catal. 117, 512-518 (1989).
[116] Moya S.A., Escudey M., J. Chem. Soc. Chem. Commun. 16, 1829-1830 (1994).
[117] Gil Llambías F.J., Escudey Castro A.M., J. Chem. Soc. Chem. Commun. 9, 478-479 (1982).
[118] Gil Llambías F.J., Escalona N., Pfaff C., Scott C., Goldwasser J., React. Kinet. Catal. Lett. 66, 225-229 (1999).
[119] Gil Llambías F.J., Escudey A.M., Fierro J.L.G., López Agudo A., J. Catal. 95, 520-526 (1985).
[120] Schwartz V., da Silva V.T., Oyama S.T., J. Mol. Catal. A 163, 251-268 (2000).

[121] Anderson J.R., García M.F., Supported Metals in Catalysis, Imperial College Press,London, Great Britain (2012).
[122] Anderson J.R., Pratt K.C., Introduction to Characterization and Testing of Cata-lysts, Academic Press, North Ryde, Australia (1985).
[123] Bautista F.M., Campelo J.M., Garcia A., Luna D., Marinas J.M., Romero A.A., Catal. Lett. 24, 293–301 (1994).
[124] Qu L., Prins R., J. Catal. 207, 286–295 (2002).
[125] Pérez-Martínez D., Giraldo S.A., Centeno A. : Appl. Catal. A 315, 35-43 (2006).
[126] Egorova M., Prins R., J. Catal. 225, 417-427 (2004).
[127] Bataille F., Lemberton J.L., Michaud P., Pérot G., Vrinat M., Lemaire M., Schulz E., Breysse M., Kasztelan S., J. Catal. 191, 409-422 (2000).
[128] Farag H., Whitehurst D.D., Mochida I., Ind. End. Chem. Res. 37, 3533-3539 (1998).
[129] Li X., Wang A., Egorova M., Prins R., J. Catal. 250, 283-293 (2007).
[130] Dufresne P., Payen E., Grimblot J., Bonnelle J.P., J. Phys. Chem. 85, 2344-2351 (1981).
[131] Okamoto Y., Imanaka T., J. Phys. Chem. 92, 7102-7112 (1988).
[132] del Arco M., Carrazán S.R.G., Rives V., Gil-Llambíaz F.J., Malet P., J. Catal. 141, 48-57 (1993).
[133] Xie Y., Tang Y.,Adv. Catal., 37, 1-10 (1990).
[134] Okamoto Y., Arima Y., Nakai K., Umeno S., Katada N., Yoshida H., Tanaka T., Yamada M., Akai Y., Segawa K., Nishijima A., Matsumoto H., Niwa M., Uchijima T., Appl. Catal. A 170, 315-328 (1998).
[135] Srinivasan R., Liu H.C., Wehler S.W., J. Catal, 57, 87-95 (1979).
[136] Goula M.A., Kordulis Ch., Lycourghiotis A., J. Catal. 133, 486-497 (1992).
[137] Goula M.A., Kordulis Ch., Lycourghiotis A., Fierro J.L.G., J. Catal. 137, 285-305 (1992).
[138] Hanika J., Janoušek V., Sporka K., Collect. Czech. Chem. Commun. 52, 663-671 (1987).
[139] Okamoto Y., Umeno S., Arima Y., Nakai K., Takahashi T., Uchikawa K., Inamura K., Akai Y., Chiyoda O., Katada N., Shishido T., Hattori H., Hasegawa S., Yoshida H., Segawa K., Koizumi N., Yamada M., Nishijima A., Kabe T., Ishihara A., Isoda T., Mochida I., Matsumoto H., Niwa M. and Uchijima T., Appl. Catal. A 170, 343-357 (1998).
[140] Bergwerff J.A., Visser T., Leliveld B.R.G., Rossenaar B.D., de Jong K.P., Weckhuysen B.M., J. Am. Chem. Soc. 126,14548-14556 (2004).
[141] Van de Water L.G.A., Bergwerff J.A., Niijhuis T.A., de Jong K.P., Weckuysen B.M., J. Am. Chem. Soc. 127, 5024-5025 (2005).
[142] Van de Water L.G.A., Bergwerff J.A., Leliveld B.R.G., Weckhuysen B.M., de Jong K.P., J. Phys. Chem. B 109, 14513-14522 (2005).
[143] Bergwerff J.A., Jansen M., Leliveld B.R.G., Visser T., de Jong K.P., Weckhuysen B.M., J. Catal. 243, 292-302 (2006).
[144] Bergwerff J.A., Visser T., Weckhuysen B.M., Catal. Today 130, 117-125 (2008).
[145] Bergwerff J.A., van de Water L.G.A., Visser T., de Peinder P., Leliveld B.R.G., de Jong K.P., Weckhuysen B.M., Chem. Eur. J. 11, 4591-4601 (2005).
[146] Beale A.M., Jacques S.D.M., Bergwerff J.A., Barnes P., Weckhuysen B.M., Angew. Chem. Int. Ed. 46, 8832-8835 (2007).
[147] Lysova A.A., Koptyug I.V., Sagdeev R.Z., Parmon V.N., Bergwerff J.A., Weckhuysen B.M., J. Am. Chem. Soc. 127, 11916-11917 (2005).
[148] Da Silva P., Marchal N., Kasztelan S., Stud. Surf. Sci. Catal. 106, 353-360 (1997).
[149] Pratt K.C., Sanders J.V., Christov V., J. Catal. 124, 416-432 (1990).
[150] Vaudry F., Khodabandeh S., Davis M.E., Chem. Mater. 8, 1451-1464 (1996).
[151] Bagshaw S., Pinnavia T.J., Angew. Chem., Int. Ed. Eng. 35, 1102-1105 (1996).
[152] Zhang W., Chem. Commun. 1185-1186 (1998).
[153] Čejka J., Žilková N., Rathouský J., Zukal A., Phys. Chem. Chem. Phys. 3, 5076-5081 (2001).
[154] Stoepler W., Unger K.K., Stud. Surf. Sci. Catal. 16, 643-651 (1983).
[155] Jirátová K., Janáček L., Schneider P., Stud. Surf. Sci. Catal. 16, 653-663 (1983).
[156] Zakcharchenya R.I., J. Sol-Gel Sci. Techn. 6, 179-186 (1996).
[157] Kemp R.A., Adams C.T., Appl. Catal. A 134, 299-317 (1996).

[158] Campa M.C., Cerrato G., Chiorino A., Gazzoli D., Ghiotti G., Indovina V., Prinetto F., J. Phys. Chem. 99, 5556-5567 (1995).
[159] Pizzio L., Vázquez P., Cáceres C., Blanco M., Stud. Surf. Sci. Catal. 127, 413-420 (1999).
[160] Vrinat M., Hamon D., Breysse M., Durand B., Des Courieres T., Catal. Today 20, 273-282 (1994).
[161] Afanasiev P., Geantet C., Breysse M., J. Catal. 153, 17-24 (1995).
[162] Maity S.K., Rana M.S., Bej S.K., Ancheyta-Juárez J., Murali Dhar G., Prasada Rao T.S.R., Appl. Catal. A 205, 215-225 (2001).
[163] Dzwigaj S., Louis C., Breysse M., Cattenot M., Bellière V., Geantet C., Vrinat M., Blanchard P., Payen E., Inoue S., Kudo H., Yoshimura Y., Appl. Catal. B 41, 181-191 (2003).
[164] Vrinat M., Letourneur D., Bacaud R., Harlé V., Jouguet B., Leclercq C., Stud. Surf. Sci. Catal. 127, 153-160 (1999).
[165] Boehm H.P., Stud. Surf. Sci. Catal. 48, 145-157 (1989).
[166] Abotsi G.M.K., Scaroni A.W., Fuel Process. Technol. 22, 107-133 (1989).
[167] Solar J.M., Leon Y., Leon C.A., Osseo-Asare K., Radovic L.R., Carbon 28, 369-375 (1990).
[168] Solar J.M., Derbyshire F.J., de Beer V.H.J., Radovic L.R., J. Catal. 129, 330-342 (1991).
[169] Radovic L.R., Rodriguez-Reinoso F., Carbon materials in catalysis, Thrower P.A. (Ed.), Chemistry and physics of carbon, vol. 25, pp. 243-358, Dekker, New York, (1997).
[170] Jagiello J., Schwarz J.A., J. Colloid. Interface. Sci. 154, 225-237 (1992).
[171] Klicpera T., Zdražil M., Appl. Catal. A 216, 41-50 (2001).
[172] Cesano F., Bertaione S., Piovano A., Agostini G., Rahman M.M., Groppo E., Bonino F., Scarano D., Lamberti C., Bordiga S., Montanari L., Bonoldi L., Millini R., Zecchina A., Catal. Sci. Technol. 1, 123-136 (2011).
[173] Xu C.C., Su H., Ghosh M., Energ. Fuel 23, 3645-3651 (2009).
[174] Al-Dalama K., Stanislaus A., Energ. Fuel. 20, 1777-1783 (2006).
[175] Debecker D.P., Stoyanova M., Rodemerck U., Eloy P., Leonard A., Su B., Gaigneaux E. M., J. Phys. Chem. C, 114 18664-18673 (2010).
[176] Leyrer J., Mey D., Knozinger H., J. Catal. 124, 349-356 (1990).
[177] Mestl G., Srinivasan T.K.K., Cat. Rev. Sci. Eng. 40, 451-570 (1998).
[178] Breysse M., Afanasiev P., Geantet C., Vrinat M., Catal. Today 86, 5-16 (2003).
[179] Kučera E., J. Chromatogr. 19, 237-248 (1965).
[180] Schneider P. Chem. Eng. Sci. 39, 927-929 (1984).
[181] Šolcová O., Soukup K., Schneider P., Micro. Meso. Mat. 91, 100-1006 (2006).